C.P. No. 230
(17,696)
A.R.C. Technical Report

C.P. No. 230
(17,696)
A.R.C. Technical Report

MINISTRY OF SUPPLY

AERONAUTICAL RESEARCH COUNCIL

CURRENT PAPERS

Development of an Air Mass-Flow Rate Meter

By

W. J. G. Cox, A.M.I.E.E., A.M.A.I.E.E.

LONDON: HER MAJESTY'S STATIONERY OFFICE

1956

PRICE 4s. 6d. NET

C.P. No. 230

U.D.C. No. 532.57

Technical Note No. Instn 142

October, 1954

ROYAL AIRCRAFT ESTABLISHMENT

Development of an Air Mass-Flow Rate Meter

by

W.J.G. Cox, A.M.I.E.E., A.M.A.I.E.E.

SUMMARY

The development of an Air Mass Flow rate meter to cover a very wide range is described which, essentially an analogue computer, gives a two-sweep pointer direct presentation of air mass flow rate, independent of pressure, temperature and velocity changes within the range of the instrument. The pointers are driven by a servo system which is error-actuated from the computing bridge network, secondary feedback being employed to maintain stability with a saturated angular output rate of approximately 33° per second. Specifications and performance figures are given for the individual transducer elements and the complete instrument, error estimations are made, and the servo stability is discussed.

LIST OF CONTENTS

LIST OF ILLUSTRATIONS

1 Introduction

The measurement of small air mass flow rates can be readily achieved by several methods. For instance the angular deflection of a swing plate located in the airstream is related to mass flow rate, or, alternatively, if a known small heat energy input in the air stream causes a measurable temperature rise, then the mass flow rate can be assessed from known specific heat values, as in the instrument described in reference 4. But the measurement of larger air mass flows cannot be assessed accurately by these means, and the need for an instrument giving a direct mass flow rate indication over the wide ranges used in gas turbine and compressor work has led to the development of the instrument described herein.

It was evident that the direct metering of large amounts of air was not a practical proposition, and consequently attention was turned to measuring the dependent pressures and temperature of the moving air, and correlating these in one instrumentation scheme to give the required mass flow rate.

2 Principle of measurement

In an air stream, if 'P' is the static pressure absolute, 'T' is the absolute temperature, 'ρ' and 'v' the density and velocity respectively, and 'D' is the dynamic pressure rise above the static, then from the gas equation:-

$$\frac{P}{\rho T} = \text{a constant}, \quad \text{or} \quad \rho \propto \frac{P}{T} \tag{1}$$

and as $D \propto \rho v^2$, then $v \propto \left(\frac{D}{\rho}\right)^{\frac{1}{2}}$. (2)

But the mass flow rate

$$M \propto \rho v \quad \text{or} \quad (\rho D)^{\frac{1}{2}} \tag{3}$$

and substitution for 'ρ' results in:-

$$M \propto \left(\frac{PD}{T}\right)^{\frac{1}{2}} \tag{4}$$

giving the mass flow rate in terms of measurable pressures and temperature within the limits of application of the laws stated above. This was agreed as an expression likely to give a practical mass flow rate indication with reasonable accuracy when transformed into instrument analogies. Overall limits were accordingly established as follows:-

P ..... 6 to 90 p.s.i. absolute

D ..... 0.2 to 9 p.s.i. differential

T ..... 288 to 612°K

$\frac{D}{P}$ not greater than 0.1

and accuracy of flow indication was required if possible to 1%, though up to 5% would be acceptable, these percentages being of the actual indicated

quantity, and not of the 100% value. Thus the expression $\frac{PD}{T}$ varies over the range 1.96×10^{-3} to 2810×10^{-3}, and its square root over the range 0.0442 to 1.65.

A four-bar linkage was the first method tried, the variables 'P', 'D' and 'T' being converted into "log" rotations, differentials being used to add and subtract, with a final "de-log" linkage to give the answer. The movement of the assemblies, however, was inadequate to cover the range required, and the frictional and backlash effects introduced errors too large to be acceptable.

It was then decided that an electrical method for obtaining the relationship (4) given above, over the wide range required, would be more practicable than mechanical means. There are several potentiometer networks which give either a voltage or current output proportional to the product of two resistances and inversely proportional to a third resistance, and by making suitable transducers for converting 'P', 'D', and 'T' into proportional resistances in the network, a square root scale on the output voltage or current indicator will indicate mass flow rate directly. There is also the conventional Wheatstone bridge arrangement of four resistances, which, when balanced has one arm proportional to the product of the adjacent two resistances and inversely proportional to the fourth, and here again the square root of the resistance value will indicate mass flow rate. The potentiometer circuits suffer from the disadvantage that several indicators would probably be required to cover the range, and stabilised current or voltage sources would be necessary, also functioning over a wide range. The bridge circuit by comparison gives a balanced indication independent of applied voltage, and the final presentation, being the representation of a varying resistance, offers greater scope for scale extension than the current or voltage indication required by the potentiometer circuits. It was therefore decided to use the bridge arrangement, and Figure 1 gives a diagrammatic representation of the scheme adopted.

3 Method of measurement

The computing network consists essentially of four resistances as shown, arranged as the arms of a Wheatstone bridge. The static pressure in the ducting is communicated to the Static Pressure Transducer, which is a pressure-tight chamber containing an evacuated spring loaded metallic bellows. Assuming a constant spring rate, the free end of this bellows moves in proportion to any change in the absolute static pressure and this movement is made to operate a variable resistance also housed inside the chamber. This resistance, called 'A', forms one arm of the bridge and varies therefore proportionally with the static absolute pressure.

The dynamic pressure differential existing between the pitot tube and static is connected to a second pressure-tight chamber, the Dynamic Pressure Transducer. The differential pressure acts across a spring-loaded metallic bellows, the movement of which operates a variable resistance 'C' in a similar manner to the static pressure transducer. This resistance 'C' therefore varies proportionally with the dynamic pressure differential, and forms the bridge arm opposite to 'A'.

The third arm of the bridge called 'B' consists of a length of platinum wire immersed in the air stream to sense any temperature variations, any such changes resulting in a nearly proportional resistance change of the wire over the limited range in use.

The fourth arm of the bridge is the "answer" arm called 'X', and with the bridge balanced the well known relationship gives:-

$$X = \frac{AC}{B} = \frac{FD}{T} \times \text{a constant} = M^2 \times \text{a constant} . \qquad (5)$$

The balanced value of the arm 'X' which, as shown above, varies proportionally with the square of the mass flow rate, is varied automatically by a servo mechanism which in turn responds to the out-of-balance error signal across the bridge arising from any variations of 'A', 'B' or 'C' from the balanced condition. The servo tends to alter 'X' back into a balanced position where the error signal is reduced to zero and 'X' again indicates 'M^2'. The resistance 'X' is wound in the form of two uniform toroids, variation being obtained by using contact wiper arms rotatable over the windings. Attached to each wiper arm spindle is a pointer, the angular displacement of which (when the bridge is balanced) is proportional to 'X' or, in other words, to 'M^2'. By making those pointers move over a square root scale the final steady state indication of '$\sqrt{X}$' or 'M' is obtained directly. The two toroidal tracks into which 'X' has been wound form an extended range, the one covering an approximate range of 2.5% to 20% and the other from 20% to 100% of full scale. Associated with each track is its own indicator pointer, scale, and servo motor, with automatic limit switch transference between the tracks so that the servo system can seek to establish a balance point over both tracks. This two sweep presentation enables the required range to be covered within a reasonable dial dimension, and gives adequate "readability" at the low end of the scale.

4 Description

4.1 General

Figures 2, 3 and 4 give general views of the instrument with the covers removed. The components are mounted within a rectangular alloy-angle frame, the front end of which carries the display dial and indicator pointers. Mounted off the rear of the dial plate are the servo motor assemblies with their gear and worm drives to the 'X' tracks and display pointers. Behind this assembly are mounted the static and dynamic pressure transducers housing the variable resistance mechanisms responsive to the static and dynamic pressures respectively.

Located on the right hand side is an "electrical controls" panel, on which is mounted a double-wound moving coil relay (responsive to error signals from the main computing bridge), the preset test control switches, feedback and sensitivity controls, and all the relays necessary for the servo system operation.

The power supply pack is located at the rear end of the frame and contains a step-down transformer, rectifiers and smoothing condensers for supplying electrical power to the bridge network and servo mechanism control circuitry. The illustrations also show a sub-panel mounted above the power pack and carrying two pressure gauges registering the dynamic and static pressures. These are for test purposes only and are not part of the instrument.

4.2 Static pressure transducer

Figure 5 illustrates this transducer. The entire mechanism is contained within a cylindrical pressure shell of brass, with flanged and bolted end plates, the interior assembly being pillar-mounted off the base-plate flange. An evacuated and sealed metallic bellows (containing an inner compression spring coaxial with the bellows) is located between the pillar supports, and is secured to the base-plate by three individual clamps in order to facilitate lining-up.

The upper free end of the bellows assembly carries a push-rod which is coaxial with the bellows, and is located between upper and lower guide rollers, ensuring that only linear vertical motion of the bellows and push-rod takes place. The middle section of the push-rod is formed into a rack which engages with a pinion shaft, in turn mounted at each end on ball bearings. This pinion shaft carries a clamped wiper arm assembly which makes contact with, and moves over, the inner surface of a toroidal resistance track. This resistance forms the 'A' arm of the bridge, and is carried in an insulated ring housing, the centre of which is coincident with that of the pinion shaft. The wiper arm contact is insulated from the arm, and connection is made through a wire passing through a hole drilled down the centre of the pinion shaft.

All the electrical connections are led through hermetic ceramic seals soldered into the base plate. A vibrator assembly comprising a small motor and eccentrically-mounted mass is shown fixed adjacent to the pinion shaft, and was initially fitted in case the stiction between the wiper brush and track should prove to be excessive and some vibration be required to free the motion. After tests, however, it was evident that vibration would not be required.

4.3 Dynamic pressure transducer

This unit is shown in Figure 6. As in the case of the static pressure transducer, a cylindrical brass shell with flanged and bolted end plates forms the pressure-tight container for the mechanism. The static pressure is communicated to this shell which also contains an inner housing for a spring-loaded metallic bellows. The bellows is soldered around its top edge to this inner housing, the bottom end of the bellows being free to move vertically. The dynamic pressure is connected to the inner housing and acts on the outside of the bellows to move the bottom upwards against the static pressure acting inside the bellows.

A push rod extends from the bottom of the bellows up through a large clearance hole in the top of the inner housing, and terminates in a rack profile. Roller guides are arranged along the length of the push-rod to ensure that truly vertical motion only is possible. The rack engages with a pinion shaft, ball-bearing mounted as shown, which in a similar manner to the static pressure transducer carries a wiper arm, capable of moving over the inner surface of a toroidal resistance track. This resistance forms the 'C' arm of the main bridge. As previously described, hermetic ceramic seals passing through the shell are used to enable external electrical connections to be made.

4.4 Temperature sensitive element

The element used in the air duct is the standard impact bulb type IT 3-2. This element is of platinum wire wound over an open insulated former and is presented axially to the air stream. A tubular shroud with a frontal opening surrounds the element, and the air passing over the element escapes through small side holes at the rear end of the shroud. These holes are sized so that total stagnation of air around the element is avoided without permitting a high enough speed to introduce an appreciable velocity head error. For temperatures higher than some 120°C the insulation of the standard head is modified to more suitable high temperature material.

4.5 Dial plate, servo motors and drive assembly

Figure 7 gives a general view of this assembly. The dial plate is of light alloy and carries in the front a central bossed opening through

which project the concentric drive shafts for the pointers. These pointers move over inner and outer scales, respectively covering the 2.5% - 20% and 20% - 100% ranges, the outer scale being some 10½ inches diameter. Only one pointer can be in the indicating zone for reading at any particular time, but to avoid confusion a small masked section of the dial (see Figure 2) is located at the top, behind which rests the particular pointer not in use. Just inside the two indicator scales is engraved a 2° interval scale for alignment and calibration use. The scales and front are of black anodised aluminium, the indications being engraved through to the bright metal underneath. A disc of perspex, rim mounted off the scale edge, forms a dust-proof protection through which the pointer display can be observed.

Behind the dial plate is located the servo motors and drives assembly. This is a two stage or two tier assembly, the inner tier (against the inside of the dial plate) comprising the 2.5% - 20% range of the 'X' resistance track, its rotating wiper and gearing; and the outer tier being the 20% - 100% range of the 'X' track with its appropriate components. The 2.5% - 20% track is wound toroidally, and its insulated housing bolted directly to the back of the dial plate. A centrally-located hollow spindle carried the wiper for this track, the connection being made through a helical spring to an insulated pillar as shown. Driving the wiper spindle is a 48:1 worm reduction drive which in turn is driven by a 9:1 spur gear reduction off the servo motor armature, giving an overall reduction of 432:1. The servo motor is the low inertia D.C. type now made by Messrs Electro Methods Ltd., and consists of an armature wound on a light hollow former, rotating around a fixed soft iron core, the field being of the high stability permanent magnet type. The hollow spindle described above is mounted at each end in ball bearings, and a reduced section of the spindle projects through the front bearing to carry the indicator pointer for the 2.5% - 20% range.

The second tier of the assembly comprises the 20% - 100% range of the 'X' track, and the mechanism layout is very similar to that of the lower range just described. The wiper spindle in this case is solid and extended in the front to pass through the hollow spindle of the lower range wiper, projecting through the dial boss to carry its indicating pointer. The connection to this wiper is made by a wire passing through a small hole drilled along the centre of the spindle at the back.

Both wiper spindles carry striker arms, which, at the extremities of the ranges operate limit switches of the micro type. These switches effect the transference from one track to the other and also switch off the servo motors at the 100% and 2.5% positions to prevent over-run.

4.6 Electrical controls panel

The circuit control components are mounted on this panel (see Figure 4). At the base is located the double-wound moving coil relay. This is a type S.54 instrument made by Messrs Sangamo Weston and contains two control windings - one used for sensing any out-of-balance of the bridge, and the other carrying a feed-back signal from the servo motor circuit. Above this relay are placed the test switches for checking the positioning of the pointers on each range, and the rheostat controls for adjusting the bridge sensitivity and amount of secondary feed-back. At the top of the panel are mounted the control relays, which are of the high speed type with changeover contacts.

The back of the panel has, at the top end, a terminal strip for interconnection to the bridge and power pack, and also carries two preset resistances used as test arms of the bridge for repositioning the pointers. Rectifier type suppressors are soldered directly to the connecting stalks of the relays.

4.7 Power pack

A standard service type power transformer with multi-stepdown windings supplies electrical power for the circuitry. The mains input winding is suitable for 230/250 volt, single phase, 50 cycles A.C. Selenium type half-wave rectifiers with electrolytic smoothing condensers provide individual smoothed D.C. inputs to the bridge and control circuit respectively, and also included is a separate rectified and switched supply for the vibrator motor of the Static Pressure Transducer mentioned in paragraph 4.2.

5 Control Scheme

5.1 Description

The wiring diagram of the control scheme is shown in Figure 8. As already explained, the main bridge is comprised of the variable resistances 'A', 'B' and 'C' (responsive to static pressure, temperature and dynamic pressure respectively) and the servo driven variable resistance 'X', the value of which is indicated by the angular position of pointers and, when balanced, gives the mass flow rate answer. In series with each of the 'A', 'B' and 'C' resistances are small padding resistances, the values of which are arranged to bring the calibration lines through the true origin (see Figures 13, 14, 15). A three-pole changeover "test" switch is fitted so that in the "normal" position the resistances 'A', 'B' and 'C' are in circuit, while in the "test" position pre-set resistances are switched in making a definite balanced value of 'X' available for repositioning of the pointers. A "test range selector" switch operates on one of the pre-set resistances making this balanced value position available on both the high and low ranges.

The supply to the bridge is taken through the "free" end of the 'X' arm so that a progressively higher resistance is placed in series with the bridge as it closes down to lower resistance levels, and tends to counteract the increasing sensitivity of the bridge. At the lower end of the high range 'X' track the sensitivity requires still further reduction, and a 4,700 ohm series resistance in this arm, which is normally short-circuited, is placed in circuit by the opening of a switch operated by a striker arm on the wiper of the high range track. When indication is switched to the "low range" 'X' track, a range transfer relay No.3 is arranged so that its contacts change over the bridge supply from the high range track through to a pre-set sensitivity control variable resistance in series with the low range track. The one setting of this control is found adequate for all positions in the low range, as here the rate-of-change of resistance is much less than that of the high range track.

The bridge out-of-balance is sensed by a moving coil relay. This is a type 3.54 relay made by Messrs Sangamo Weston Ltd. The contact arrangement is a changeover one, with a central contact moved by the armature between two limiting fixed contacts. In the central position with no armature current flowing the contacts are open-circuited, and this position is held stable by the armature control spring. The armature is double-wound, one of the windings (called the sensing coil) being connected across the bridge to sense any out-of-balance. If an out-of-balance current of the order of 5 micro-amps flows the armature is deflected and contact made either one side or the other depending upon the direction of the out-of-balance current. The second winding (called the feedback coil) obtains a pre-set controlled current only while either servo-motor is energised, and is arranged directionally so that it acts on the relay armature in opposition to the sensing coil.

The contacts of the moving coil relay control two high speed relays, the "Increase" and "Decrease" relays respectively, the changeover contacts of which switch the supply on to the servo-motors directionally so that with the "Increase" relay "on", the servo-motor rotates to increase the 'X' resistance, while opposite rotation occurs with the "Decrease" relay "on". Both relays cannot be energised simultaneously, and when de-energised the servo-motors are short-circuited. "High" and "low" limit switches are wired into the "Increase" and "Decrease" relay coil circuits. These switches are open-circuited by strikers on the wiper arms of the 'X' resistance high and low ranges at the 100% and 2.5% positions respectively, and prevent over-run of the servo-motors beyond these limits.

Range Transfer Switches are located at the top end of the low range track and the bottom end of the high range track. These are operated by strikers on the wiper arms, and control the high speed range transfer relays to ensure that the appropriate servo-motor changeover sequence is observed when running through from one range to the other. Over the region of operation of these switches the track winding resistance turns are shorted together so that the changeover action takes place without a change of resistance of the 'X' arm.

The feedback coil of the moving coil relay is connected in series with a controlling resistance across the servo-motor supply and carries a current only while the servo-motors are energised, this current being reversed on reversal of motor rotation. As stated above, the polarity of the feedback coil is arranged in opposition to that of the sensing coil.

5.2 Functioning

An analysis of the system is given in Appendix I, and the following paragraphs give a verbal description.

Assuming for the moment that the feedback circuit is not connected, Figure 9 illustrates the transient behaviour of the servo system components when subjected to a step function input disturbance. In this diagram 'θ_i' is the input or the desired angular position of the 'X' track wiper arm, and 'θ_o' is the output or actual angular position of the arm. (Figure 9a shows their transient behaviour.) 'θ_e' is the error, or difference between input and output, and is depicted in Figure 9b. Figure 9c shows the variation of the current in the moving coil relay sensing coil, and Figure 9d the angular movement of the relay armature. The contact arrangement consists of two leaf springs fixed to the armature and these constitute the moving contact. Fixed point contacts are located each side of the moving contact so that a displacement of $\pm \psi_o$ has to take place before contact is made. Further displacement can take place between ψ_o and ψ_1 values on each side and over these regions the contact spring is being compressed. At the $\pm \psi_1$ positions the armature stop prevents further movement outside these limits. Thumbnail sketches in Figure 9d indicate the attitude of the armature at various instants. Figure 9e shows the rate of error correction, $\frac{d\theta_e}{dt}$.

Prior to instant "t_{01}", the error, error rate and sensing coil current are assumed zero, with the bridge balanced and the relay armature central, and further assuming that balance is occurring on the high range, the low range servo-motor will be shorted out by Transfer Relay No.2 (Figure 8), and Relay No.1 will hold the high range servo-motor in circuit. At instant "t_{01}", one of the bridge arms is given a step change resulting in a sudden increase of 'θ_i' to a new value, assumed to be large. The unbalance of the bridge results in a sudden increase from zero of the

sensing coil current, which deflects the relay armature so that at instant 't_{02}' contact is made at the '$+\psi_o$' position and the "Increase" relay is energised. This starts up the high range servo-motor which in turn moves the 'X' resistance track wiper and starts to increase 'θ_o' up towards the 'θ_i' value. As shown by the Figure 9e the servo-motor soon saturates to a constant speed, giving a uniform error correction rate.

After initial contact at 't_{02}' the relay armature further deflects until brought to rest against its stop at the 'ψ_1' position, and this position is maintained until the sensing coil current (which is progressively falling as error correction proceeds) falls to a value 'i_1', which would just maintain the relay armature deflection at 'ψ_1' in the steady state. At this instant 't_{03}' the armature begins to move back towards a central position, and at instant 't_{04}' again reaches the '$+\psi_o$' position where contact is broken and the "Increase" relay de-energised. The servo-motor is consequently short-circuited at this instant and rapidly slows down, causing the "error" and sensing coil current to reach the small steady state values of '$\theta_{e(s)}$' and '$i_{(s)}$' respectively.

The moving coil relay armature also eventually attains a steady state value '$\psi_{(s)}$' but as it is an independent spring-mass system assumed critically damped it may also reach a 'ψ_{min}' value (less than '$\psi_{(s)}$') at some instant 't_{05}'. If 'ψ_{min}' falls to the '$-\psi_o$' value a reverse corrective sequence will take place to reduce 'θ_o' from its overshoot value. Thus an oscillatory condition of 'θ_o' is set up, the attenuation of which will depend upon such factors as error rate and width of the '$+\psi_o$' to '$-\psi_o$' zone. The criterion for this servo-system is that the indicated output 'θ_o' should be moved to its new steady state value as quickly as possible but without any overshoot. These conditions are obviously fulfilled if 'ψ_{min}' just falls short of the '$-\psi_o$' value, and this condition is achieved progressively from the oscillatory condition by decreasing the error correction rate and/or increasing the '$+\psi_o$' to '$-\psi_o$' zone width. But increase of this zone width is undesirable as it leads to an increase in the indicated error for steady state conditions, and for reducing hysteresis of indication the zone width should be kept to a minimum.

A secondary feedback loop is introduced so that the error correction rate can be increased while maintaining a minimum dead zone and still meeting the requirement for dead beat indication without overshoot. Figure 10 shows the typical transient behaviour of the system with feedback in operation. A starting condition (prior to instant 't_{06}') is assumed where a substantial error has been established, and error correction is being effected at the saturated rate. The graphs for 'θ_i', 'θ_o' and 'θ_e' have been omitted in Figure 10, as these are all linearly interdependent, and Figure 10a shows the sensing coil current which, for small unbalances, is proportional to the error 'θ_e'.* The wiring diagram shows the feed-back coil connected through a controlling resistance in such a way that a constant current flows through it while any servo-motor is energised, this current changing in direction with reversal of drive signal to the servo-motors, and dropping to zero when the moving coil relay contacts are open. This feed-back coil current is shown in Figure 10b, and being wound in opposition to the sensing coil, the vector addition of these coil currents (to scale) produces an "effective" coil current shown in Figure 10c to which the relay armature is responsive.

At instant 't_{06}' the effective coil current has fallen to the '$+i_1$' value and the relay armature commences to move away from the '$+\psi_1$' stop. At instant 't_{07}' the armature has deflected to the '$+\psi_o$' position where the servo-motor is switched off and short circuited to retard the error correction rate. Also at instant 't_{07}' the feedback coil current is reduced to zero, giving a step increase to the effective coil current to

---

* See equation (89), Appendix I

a value equal to the sensing coil current. As this value may be substantially above the '$+i_0$' value (as shown), the relay armature movement is reversed and deflected back towards the '$+\psi_1$' region, reaching the '$+\psi_0$' position at some instant 't_{08}'. Here the servo-motor is again switched on to increase error correction rate, but at the same time the feedback current is also established giving an effective coil current tending to move the armature back towards its centre-stable position. These stages of operation are repetitive until at some such instant as 't_{09}' when the armature passes through the '$+\psi_0$' position towards zero, the sensing coil current (being equal to the effective current as the feedback coil is de-energised) is left at a value below '$+i_0$'. No further switching takes place and the transients pass to the steady state conditions depicted after instant 't_{09}'.

Thus the effect of the secondary feedback is to present a spurious balance-point to the relay armature while the main bridge is still unbalanced. This spurious balance point can be approached with a high error correction rate and as soon as near balance is achieved the true balance point of the bridge is presented intermittently to the relay for any further corrective action, the average correction rate being much less here (interval 't_{08}' to 't_{09}') due to the continual switching in and out sequence of the servo-motor described above. An increase in the feedback current, without a change of maximum error rate will lead to repetitions of intervals like 't_{08}' to 't_{09}', giving a prolongation of intermittent operation over which the average error correction rate is much less than the maximum saturated value. There is obviously no advantage in this type of operation over the single step shown in Figure 10.

Within limits an increase in the feedback current together with an increase in the error correction rate will improve the performance, but an excessive feedback can cause continuous rapid oscillation of the relay armature at bridge balance. This condition is shown in Figure 11, and is a case of the familiar oscillatory behaviour of a damped spring-mass system when a periodic forcing function is applied leading the motion by a phase angle less than 180°. It has been assumed in describing the transients of Figures 9 and 10 that the switching delay time of the "Increase" or "Decrease" relay is negligibly small compared with the duration of the other events. But where a large feedback force is available to move the damped relay armature rapidly, these delay times 'Δt' shown in Figure 11 may become an appreciable fraction of the periodic time of the resulting motion. The feedback then constitutes a forcing function leading the relay armature movement by a phase angle less than 180°, and if the amplitude of the feedback signal is large enough to equalise numerically the gradients of the Figure 11b curve at the points 'X', then oscillation will be sustained.

In normal operation the feedback current is set well below this extreme condition, and Figure 12 shows recordings of the transient behaviour of the system to step input changes. Figure 12a shows the oscillatory condition which can exist without secondary feedback at a sufficiently high error correction rate, and Figure 12b shows the stabilising effect of secondary feedback. It will be noticed that in Figure 12b the value of the feedback signal is such as to give several switched intervals of the 't_{08}' to 't_{09}' type, before a steady state is achieved. While the ideal would be just one or two as explained previously, it is not possible to preset the feedback to give this condition of operation over the whole of the bridge, due to an increase in sensitivity as the bridge arms reduce in value. Thus a setting is effected which gives the required minimum of switched steps at the low end of the bridge, and which entails a few more switched steps at the high end before a steady-state indication is reached. But this action is not noticeable visually as it will be seen from the time marks of the recording that the whole period of feedback switching is some 0.2 to 0.3 seconds, with each switch step taking approximately 1/20th of a second.

6 Design Considerations

6.1 General

As the instrument was intended for test-house use and would be static during indication, no restrictions as to size and weight were applied, and no requirement for operation under accelerated motion was applicable. A direct visual presentation of mass flow rate had to be given, preferably a pointer type of display, capable of being photographed with other test instruments to give permanent records of test runs.

6.2 Computing bridge

This was designed around two existing components - the moving-coil relay and the temperature sensitive element. The sensing coil of the relay has a resistance of 150 ohms making contact either side for a current of ± 5 microamps, while the temperature sensitive arm has the temperature/resistance characteristic shown in Figure 13. The actual law does not give a true straight line relationship, though this must be assumed to exist for computation purposes. The curve of error involved in this assumption is also given in Figure 13, showing a maximum of 0.73% in the 100°C region. A further design limitation is the maximum current permissible through the temperature element which must be kept below 15 milliamps to avoid any appreciable heating up of the element and consequent false indication of ambient temperature.

6.21 Static pressure transducer

In order that small air pressure changes should create the maximum total force changes to oppose friction effects, the largest diameter bellows procurable for the pressure range is used. This is a 2" O.D. × $1\frac{3}{8}$" I.D. hydroflex metallic bellows having 16 convolutions, rated for a maximum pressure differential of 165 p.s.i. by the makers, Messrs. Drayton Regulator and Instrument Company. The combined spring-rate of the bellows and internal spring is some 330 lb/inch, whereas that of the bellows only is 45 lb/inch. Thus the characteristic of the combination is mainly that of the spring only, and any imperfections in the bellows acting as a spring have practically no influence.

The machine-cut rack has 25.5 teeth/inch engaging with a 15-tooth pinion wheel, and the resistance winding of 39 s.w.g. oxidised Eureka is close-wound on a 3-inch diameter ring former, giving a resistance of 0.6 ohms per turn. Eureka is chosen to minimise resistance change with temperature. Figure 14 gives the calibration characteristic of the unit, and also indicates the percentage error at any particular pressure or resistance value due to the finite resistance of each turn of wire. A second source of small error may be due to the imperfect evacuation of the bellows unit, and temperature changes effecting pressure changes on the residual air contents. This effect is quite small, and calculation shows that if evacuation is carried to 3 mm Hg absolute, then a 10°C change at ordinary room ambients will effect a pressure change less than 0.002 p.s.i.

The shell and flanges are of brass, fabricated by brazing, and are made amply robust to ensure that no flexing of the material is likely to affect the angular position of the wiper brush.

6.22 Dynamic pressure transducer

In this unit also, the largest bellows available for the pressure is used. This has a $4\frac{1}{2}$" O.D. × 3" I.D. with 11 convolutions and is rated at 17 p.s.i. differential maximum. The combined spring-rate of the bellows and internal spring is 77 lb/inch and that of the bellows alone is 5 lb/inch.

A rack similar to the one in the static pressure transducer is used, engaging in this case with a 40 tooth pinion wheel. This resistance winding, again of oxidised Eureka, is of 38 S.W.G. wire, close-wound on a 5 inch diameter ring former, and has a resistance change per turn of 0.4 ohms. Figure 15 gives calibration details, including an error indication due to the discreet nature of the winding as in the case of the static pressure transducer. It will be noted that the maximum pressure attained for linear relationship is 8.4 p.s.i. whereas the initial requirement was for 9 p.s.i. maximum. The lower figure was agreed as acceptable.

6.23 Indicating ('X') tracks

As stated earlier, the 'X' arm of the bridge is divided into two tracks, one giving a balance point up to approximately 20% of full scale, and the other covering the remainder of the range. These tracks are electrically in series, each having its own servo-motor and gearing, and limit switching between them enables the balance point search to continue as required from one track to the other. To ensure that switch hysteresis or overlap does not affect the indication of the "high" track starting just where the "low" track ceases to indicate, all transference switching is done over shorted-out sections of the tracks, where resistance change is zero. The concentric arrangement adopted for bringing the indicator shafts out to the dial enables each pointer to be solidly fixed to the shaft carrying its track wiper, and gives an accurate indication of its position, avoiding possible backlash errors in gearing of alternative arrangements.

The low range track is also of oxidised Eureka, 30 S.W.G. close-wound on a 6-inch diameter ring former, and has a resistance change per turn of 0.157 ohms. Figure 16 gives details of this winding, and also shows the percentage error due to the finite resistance change per turn. Half this value is also shown plotted, giving the error related to the final square root display scale.

Figure 17 details these characteristics for the high range winding, which is of 42 S.W.G. oxidised Eureka on a $3\frac{1}{2}$-inch diameter former, having a turn-to-turn resistance change of 2.25 ohms.

6.24 Bridge sensitivity

As the bridge is used over a very wide range of variation of its arms, its sensitivity at balance is also variable when fed from a constant potential source. This increase in sensitivity as the bridge arms reduce in value enables the same "error" current to flow through the relay sensing coil for progressively smaller "error" displacements, resulting in a narrow null zone at low readings, increasing to a very wide zone at the higher indications. In the present arrangement this effect is counteracted by feeding the current into the bridge through the "free" end of the 'X' arm. As this arm balances the bridge at progressively lower values, an increasing resistance is placed in series with the bridge supply, and tends to offset the increase in sensitivity. This arrangement does not give full counteraction, but avoids the mechanical complications of the more ideal arrangement of a separate series track of a higher value, varied by its own wiper from the indicator spindle. The bridge sensitivity must be considered in conjunction with the saturated rate of the servo-motor and the amount of feedback, and further reduction of bridge sensitivity is found to be necessary at the low end of the high range. This is done by switching in an additional fixed series resistance at approximately the 30% position, the switch being operated by a striker on the resistance wiper arm. As the

maximum rate of change of resistance of the low range track is approximately 1/25th that of the high range track, a fixed series resistance is found adequate to give acceptable operation on this lower range.

6.3 Feedback

This type of "knock-off" feedback is chosen because of its simplicity over the more usual velocity or velocity-squared feedbacks[5] which would require additional components to sample the servo-motor rates for reference back to the moving coil relay. When used in conjunction with a null-point detector having a dead zone, quite acceptable performance is obtained for this class of servo, as is illustrated in Figure 12b.*

7 Calibration

Precaution was taken when preparing the static pressure transducer bellows for evacuation to boil the unit for several hours to ensure removal of the maximum amount of occluded air. After evacuation and sealing, the unit was checked for leakage over a protracted period by micrometer measurement to ensure that its behaviour as a barometric capsule was uniform.

Both pressure transducers were thoroughly exercised on test rigs which supplied slowly pulsating compressed air to the units, taking them over their full ranges. All moving parts were lubricated with molybdenum disulphide lubricant, and it was also found beneficial as a surface treatment for the resistance tracks. The dynamic pressure transducer was calibrated against a mercury 'U' tube manometer, and the static pressure transducer against a substandard gauge which in turn was checked against a deadweight calibrator. Figures 14 and 15 show the results obtained, and all points were within reading error of the linearity shown.

8 Performance

The maximum angular rate of presentation, or saturated error correction rate is 33.3° per second.

The estimation of error is complicated by the fact that the bridge is used over a wide range of sensitivities and arm values, and any particular value of the indicating (X) resistance involves a range of combinations of the variables 'A', 'B' and 'C'. Figure 18 illustrates the error distribution for the particular value of the 'X' resistance at the change-over point from the low to the high track. At this point 'X' = 220 ohms, therefore with the bridge balanced:-

$$\frac{AC}{B} = 220, \qquad \text{or} \qquad \frac{A}{B} = \frac{220}{C} \tag{6}$$

and the diagram shows all possible values of 'A', 'B' and 'C' satisfying this equation between the practical limits imposed. Each radial line drawn is for a constant value of 'C', having a slope of $220/C$ or 'A/B', thus any point in the area indicates a unique combination of 'A', 'B' and 'C' to give the result at equation (6) above. The limit curve of 'C $\pm$ 1.1 A' is imposed by the condition stated in paragraph 2, that 'D' shall not be greater than '0.1 P'.

If the quantity '$\frac{AC}{B}$' has the error '$\delta\left(\frac{AC}{B}\right)$', due to errors of '$\delta A$', '$\delta C$' and '$\delta B$' in the quantities 'A', 'C' and 'B' respectively, then the proportional error:-

* Further analytical details are contained in Appendix I.

$$\frac{\delta\left(\frac{AC}{B}\right)}{\left(\frac{AC}{B}\right)} \simeq \frac{\delta A}{A} + \frac{\delta C}{C} - \frac{\delta B}{B} \qquad (7)$$

and with each point on the diagram is associated this summation of individual proportional errors, giving a distribution of total proportional errors of the constant quantity $\frac{AC}{B} = 220$ for all variations of 'A', 'C' and 'B'.

These summated errors form contour lines over the region as shown, and give ready indication of combinations of 'A', 'C' and 'B' resulting in maximum or minimum errors. All values are taken as positive in equation (7) to give the worst case.

Another error involved is due to the finite dead zone of the moving coil relay. References (2) or (3) state a convenient form of obtaining a bridge out-of-balance current flow resulting from a small proportional change in one or more arms from the balanced value. This is:-

$$\frac{\delta R}{R} \simeq \frac{iU\left(1 + \frac{G}{W}\right)\left(1 + \frac{L}{Y}\right)}{V} \qquad (8)$$

where $\frac{\delta R}{R}$ is a small proportional change in one of the balanced arms resulting in an out-of-balance current "i"; "U" is the sum of bridge arm resistances; "G" is the sensing coil resistance; "W" and "Y" are the effective bridge resistances as viewed by the sensing coil and input points respectively; "L" is the resistance in series with the bridge; and "V" is the applied voltage across the bridge and series resistance "L".

By inserting the full dead zone current value of 10 micro-amps and the other applicable values in equation (8), the proportional parts error $\frac{\delta R}{R}$ can be obtained for each point in Figure 18. These could also be plotted as contours, though, to avoid confusion, they have been left as isolated points carrying a number indicating the $\left(\frac{\delta R}{R}\right) \times 100$ value. Maximum errors are obviously incurred where C = 50, A = 745 and B = 170 for the position X = 220.

To these errors must be added the error due to the indicating track 'X', giving a total error of:-

$$\left(\frac{\delta X}{X} + \frac{\delta R}{R} + \frac{\delta A}{A} + \frac{\delta C}{C} + \frac{\delta B}{B}\right) \times 100\% \qquad (9)$$

applicable to the final indication of the quantity $\frac{AC}{B}$. As this represents $(M)^2$, the total error applicable to the Mass Flow Rate Scale $\left\{\text{or } \sqrt{\left(\frac{AC}{B}\right)}\right\}$ is half the quantity given at (9) above.

Figure 19a shows this estimated maximum error over the full mass flow rate scale, as a percentage of the actual value of mass flow rate being indicated. Figure 19b shows the error as a percentage of the maximum mass flow rate.

9 Remarks and conclusions

Performance well within the required degree of accuracy is obtainable, as shown in Fig. 19.

As the output is a shaft rotation the system could be modified for remote indication on several different dials or scales, each calibrated for a particular air duct.

Further refinement of indication and accuracy if desired could be met by extending the indicating scale to three or more sweeps as required.

This technique may also be of use for the direct indication of fuel to air mass flow ratios.

List of Symbols

A_1, A_2 etc. = Constants of Integration

A = Bridge Arm Resistance, proportional to 'P'

B = " " " " " 'T'

C = " " " " " 'D'

D = Dynamic Pressure, absolute

E = Applied voltage to motor circuit (without feedback)

E_f = " " " " " (with feedback)

E_g = Motor Back - E.M.F.

F = Motor torque

G = Resistance of moving coil relay sensing coil (150 ohms)

H = "Specific" Resistance of 'X' Resistance High Range Track (894 ohms/rad)

i_a = Motor Armature Current

i_f = Moving coil relay feedback coil current

i = Moving coil relay sensing coil current

i_o = Value of i to maintain a steady state ψ_o position (5×10^{-6} amps)

i_1 = Value of i to maintain a steady state ψ_1 position

J_m = Effective Moment of Inertia of Servomotor System (800 gm cm^2)

J_r = Moment of Inertia of moving coil relay armature (25 gm cm^2)

List of Symbols (Contd)

k_1, k_2 etc. = Constants

L = Resistance in series with Bridge Network

M = Mass-flow rate of air

n = Ratio of feedback coil turns to sensing coil turns in moving coil relay

P = Static Pressure, absolute

R = Generalised resistance arm of bridge

R_a = Motor Armature circuit resistance (700 ohms)

r = Ratio of gearing, servomotor to indicating spindle (432/1)

S_1 = Torque Rate of moving coil relay armature centralising spring (200 dyne cms per radian)

S_2 = Torque Rate of moving coil relay contact leaf spring (6000 dyne cms per radian)

T = Temperature, absolute

t = Time

Δt = Operating delay time of motor control relays

U = Sum of bridge arm resistances (= A + B + C + X)

v = Air stream velocity

V = Applied voltage across bridge and series resistance 'L'

W = Resistance of balanced bridge as viewed by sensing coil, $\left\{= \frac{(X+A)(C+B)}{U}\right\}$

X = Bridge arm resistance giving "answer" (steady state $X = \frac{AC}{B}$)

Y = Resistance of balanced bridge, as viewed by input points $\left\{= \frac{(X+C)(A+B)}{U}\right\}$

Z_1, Z_2 etc. = Coefficients and constants

θ_i = Input, or desired angular position of 'X' resistance track wiper

θ_o = Output, or actual angular position of 'X' resistance track wiper

θ_e = $\theta_i - \theta_o$, the angular error

ψ = Angular deflection of moving coil relay armature

List of Symbols (Contd)

$\pm\psi_0$ = Angular limit of relay movement at which contact is made (± 0.008 radians)

$\pm\psi_1$ = Angular limit of relay movement (± 0.07 radians)

ω = Maximum (or saturated) value of $d\theta_e/dt$

ρ = Density of air

η = Phase angle

ξ = Phase angle

REFERENCES

No.	Author	Title, etc.
1	Rogers Hurty	Relay Servomechanisms. Trans. of the A.S.M.E., November 1950.
2	Andress	Sensitivity and Output Formula for Resistance Bridges. Communications and Electronics of the A.I.E.E., May 1950.
3	Andress	Improved Solutions of the Unbalanced Bridge Circuit. Rev. Sci. Inst., February 1953.
4	Stickles Sizer	Hot Wire Anemometer for Measurement of Small Air Flows. RAE Tech Note No. EL 50.
5	Uttley Hammond	Stabilization of ON-OFF Controlled Servomechanisms. Paper in "Automatic and Manual Control", Ed. Tustin.

APPENDIX I

Analysis of servo system

1 General

This analysis seeks to demonstrate the improvement effected by using this type of secondary 'knock-off' feedback.

The requirement for this servo system is that, for any step function change of any of the variables, the pointer should move reasonably quickly to indicate the new value without any overshoot. It is assumed in this analysis that the changeover time delay of the control relays, being of the order of 2 milliseconds, is negligibly small in comparison with the duration of the other sequences.

The normal method of analysing on-off servo systems is by phase-plane representation[1,5], i.e. plotting error 'θ_e' against error rate '$\frac{d\theta_e}{dt}$', or, for the moving coil relay, plotting displacement 'ψ' against '$\frac{d\psi}{dt}$'. As this may not be familiar to the general reader, and time representation and coincidences are not directly appreciated on such diagrams, this method has not been used. Its advantages are particularly apparent where a damped oscillatory transient of 'θ_e' is permitted in response to a step change, but in the case of dead-beat operation a straightforward time analysis is equally effective.

The functioning of the system is described in paragraph 5.2 and Figures 9 and 10, and this analysis is related to the sequences shown in these diagrams. It will be useful to study first the system behaviour without feedback.

2 Without Feedback

In the motor system, the torque developed is proportional to the armature current, as the permanent magnet flux is constant. Thus:-

$$F = k_1 i_a \quad \ldots \ (= 2 \times 10^6 \times i_a \text{ dyne cms}) . \tag{10}$$

Also

$$E_g = rk_2 \frac{d\theta_o}{dt} \quad \ldots \ (= 432 \times 0.0875 \frac{d\theta_o}{dt} \text{ volts}) \tag{11}$$

and

$$E = E_g + i_a R_a = E_g + 700\, i_a . \tag{12}$$

From (12),

$$i_a = \frac{(E - E_g)}{700} \tag{13}$$

and from (10),

$$F = 2 \times 10^6 \frac{(E - E_g)}{700} \tag{14}$$

or

$$F = \frac{2 \times 10^4}{7} E - \frac{2 \times 10^4 \times 432 \times 0.0875}{7} \frac{d\theta_o}{dt} . \tag{15}$$

Relating torque to the moment of inertia and angular acceleration:-

$$F = J_m \frac{d^2\theta_o}{dt^2} = 800 \frac{d^2\theta_o}{dt^2} \qquad (16)$$

and from (15) and (16):-

$$\frac{d^2\theta_o}{dt^2} + 135 \frac{d\theta_o}{dt} - 3.57\,E = 0 . \qquad (17)$$

From definition:-

$$\left.\begin{aligned} \frac{d\theta_e}{dt} &= \frac{d\theta_i}{dt} - \frac{d\theta_o}{dt} \\ \text{and} \qquad \frac{d^2\theta_e}{dt^2} &= \frac{d^2\theta_i}{dt^2} - \frac{d^2\theta_o}{dt^2} . \end{aligned}\right\} \qquad (18)$$

Assuming idealized step functions, $\frac{d\theta_i}{dt}$ and $\frac{d^2\theta_i}{dt^2}$ are zero over the transients. Substitution of (18) in (17) gives:-

$$\frac{d^2\theta_e}{dt^2} + 135 \frac{d\theta_e}{dt} + 3.57\,E = 0 . \qquad (19)$$

Integration of this equation gives:-

$$\frac{d\theta_e}{dt} = A_1 e^{-135t} - \frac{3.57}{135} E \qquad (20)$$

$$\text{and} \qquad \theta_e = -\frac{A_1}{135} e^{-135t} - \frac{3.57}{135} Et + A_2 \qquad (21)$$

giving error rate and error angle respectively. It will be noted that the exponential term tends to zero on increase of time, and the saturated, or maximum error rate tends to:-

$$\left(\frac{d\theta_e}{dt}\right)_{(max)} = -2.645 \times 10^{-2} E = -\omega . \qquad (22)$$

In the bridge circuit, when the arms are in near balance[2,3]:-

$$i = \frac{V \cdot \delta X}{XU\left(1 + \frac{G}{W}\right)\left(1 + \frac{L}{Y}\right)} . \qquad (23)$$

From definition, where θ_e is small:-

$$H\theta_e = \delta X, \quad \text{or} \quad 894\,\theta_e = \delta X . \qquad (24)$$

Considering the balanced bridge at its most sensitive position at the minimum end of the high range track where R is 220 ohms as detailed in Fig.18, these values can be inserted into (23) and (24), giving:-

$$i = 0.001146\ e_c \ . \qquad (25)$$

Behaviour of the moving coil relay armature is dependent on the torque due to this current, its moment of inertia, and the torques due to the damping forces, the centralizing spring of the armature, and the contact leaf spring.

Let

$k_4 i$ = torque due to sensing coil ($= 3.2 \times 10^5 i$ dyne cms)

$S_1 \psi$ = " " " centralizing spring ($= 200\psi$ dyne cms)

$S_2(\psi - \psi_o)$ = " " " contact spring, acting only for $+\psi_1 > \psi > \psi_o$ and $-\psi_1 < \psi < -\psi_o$ ($= 6000(\psi - \psi_o)$ dyne cms).

As velocity damping is applicable to this movement, let torque due to this factor be

$$k_6 \frac{d\psi}{dt} \ .$$

Relating these torques to the resultant motion:-

$$k_4 i - S_1 \psi - k_6 \frac{d\psi}{dt} = J_r \frac{d^2\psi}{dt^2}$$

or

$$\frac{d^2\psi}{dt^2} + \frac{k_6}{J_r}\frac{d\psi}{dt} + \frac{S_1}{J_r}\psi = \frac{k_4}{J_r} i \ , \quad \text{for} \quad +\psi_o > \psi > -\psi_o . \qquad (26)$$

Assuming that the movement is critically damped,

$$\frac{1}{4}\left(\frac{k_6}{J_r}\right)^2 = \frac{S_1}{J_r} \ \ldots \ (= 8\ \text{sec}^{-2}) \qquad (27)$$

and equation (26) becomes:-

$$\frac{d^2\psi}{dt^2} + 2\sqrt{8}\frac{d\psi}{dt} + 8\psi = 1.28 \times 10^4 i \ , \quad \text{for} \quad +\psi_o > \psi > -\psi_o . \qquad (28)$$

For motion between ψ_o and ψ_1 limits, the torque due to S_2 is also acting, and:-

$$\frac{d^2\psi}{dt^2} + 2\sqrt{\frac{S_1}{J_r}}\frac{d\psi}{dt} + \frac{S_1 + S_2}{J_r}\psi = \frac{k_4}{J_r} i + \frac{S_2}{J_r}\psi_o \ . \qquad (29)$$

This becomes:-

$$\frac{d^2\psi}{dt^2} + 2\sqrt{8}\frac{d\psi}{dt} + 248\psi = 1.28 \times 10^4 i + 1.92 \ . \qquad (30)$$

For the steady state condition, $\frac{d\psi}{dt}$ and $\frac{d^2\psi}{dt}$ are zero, and at $\psi = +\psi_1$ .. (= 0.07 radians) where $i = i_1$:-

$$i_1 = 12.05 \times 10^{-4} \text{ amps} . \qquad (31)$$

Following the sequence depicted in Fig.9 and already described, prior to instant t_{03}, the moving coil relay armature is stationary at its "$+\psi_1$" position, with error correction proceeding at its maximum rate. The bridge out-of-balance current "i" is also being reduced, and its exact value is unimportant while a large error exists, but as the bridge reaches near-balance, this current "i" becomes related to the error "θ_e" by equation (25), and it is assumed that this equation holds when, at instant "t_{03}" the current "i" has fallen to its "i_1" value (see equation 31) where the relay armature just starts to move off its $+\psi_1$ stop. At a subsequent instant t_{04} the relay armature has moved to its $+\psi_0$ position, and over the interval "t_{03}" to "t_{04}" its motion is in accordance with equation (29) or (30). For this interval, "t_{03}" can be regarded as $t = 0$, and the current during this interval is given by:-

$$i = i_1 - t \left| \frac{di}{dt}_{(max)} \right| ,$$

which, from equations (22), (25) and (31) becomes:-

$$i = 12.05 \times 10^{-4} - 3.03 \times 10^{-5} \text{ Et} . \qquad (32)$$

Substituting this value into equation (30) gives:-

$$\frac{d^2\psi}{dt^2} + 2\sqrt{8}\frac{d\psi}{dt} + 248 = 17.34 - 0.388 \text{ Et} . \qquad (33)$$

Solving this equation gives:-

$$\psi = A_3 e^{-\sqrt{8}t} \sin\{\sqrt{240}t + \eta\} - 1.565 \times 10^{-3}\text{Et} + 3.57 \times 10^{-5}\text{E} + 0.07 \qquad (34)$$

and:-

$$\frac{d\psi}{dt} = -A_3 e^{-\sqrt{8}t} \sqrt{248} \sin\{\sqrt{240}t + \eta - \xi\} - 1.565 \times 10^{-3} \text{ E} \qquad (35)$$

where

$$\xi = \tan^{-1}\sqrt{\left(\frac{240}{8}\right)} = 1.389 \text{ radians} .$$

Substituting the conditions at t_{03}, where $t = 0$, $\frac{d\psi}{dt} = 0$, and $\psi = 0.07$:-

$$\left.\begin{aligned} A_3 &= 1.012 \times 10^{-4} \text{ E}, \\ \text{and} \quad \eta &= -0.361 \text{ radians} \end{aligned}\right\} \qquad (36)$$

and equations (34) and (35) can now be written:-

$$\psi = E\left\{1.012 \times 10^{-4}\, e^{-\sqrt{8}t} \sin\left(\sqrt{240}t - 0.361\right) - 1.565 \times 10^{-3}t + 3.57 \times 10^{-5}\right\} + 0.07 \qquad (37)$$

$$\frac{d\psi}{dt} = -E\left\{1.012 \times 10^{-4} \sqrt{248}\, e^{-\sqrt{8}t} \sin\left(\sqrt{240}t - 1.75\right) + 1.565 \times 10^{-3}\right\} \qquad (38)$$

describing the relay motion over the interval t_{03} to t_{04}. If this interval is called t_{34}, then, at instant t_{04}, $\psi = +\psi_0 = 0.008$, and $\frac{d\psi}{dt} = \frac{d\psi}{dt}_{(t_{04})}$; and substitutions into equations (37) and (38) give the following relationships:-

$$E\left\{1.012 \times 10^{-4}\, e^{-\sqrt{8}t_{34}} \sin\left(15.49\, t_{34} - 0.361\right) - 1.565 \times 10^{-3}\, t_{34} + 3.57 \times 10^{-5}\right\} + 0.062 = 0 \qquad (39)$$

and

$$\frac{d\psi}{dt}_{(t_{04})} = -E\left\{1.012 \times 10^{-4} \times 15.75\, e^{-\sqrt{8}t_{34}} \times \sin\left(15.49t_{34} - 1.75\right) + 1.565 \times 10^{-3}\right\}. \qquad (40)$$

Instant t_{04} can now be regarded as the beginning of a new transient period during which the motor slows down to a standstill. For this period $t = 0$ at t_{04}, and if $i_{(04)}$ is the value of i at this instant, from equation (32),

$$i_{(04)} = 12.05 \times 10^{-4} - 3.03 \times 10^{-5}\, E\, t_{34} \qquad (41)$$

and from equation (25),

$$\theta_{e_{(04)}} = \frac{i_{(04)}}{0.001146}. \qquad (42)$$

For this period E is now zero and the motor is short-circuited. The descriptive equation for the error, from (19) now becomes:-

$$\frac{d^2\theta_e}{dt^2} + 135\frac{d\theta_e}{dt} = 0. \qquad (43)$$

Integration gives:-

$$\frac{d\theta_e}{dt} = A_1\, e^{-135t} \qquad (44)$$

and

$$\theta_e = -\frac{A_1}{135}\, e^{-135t} + A_2. \qquad (45)$$

Inserting the known conditions at t_{04} where $t = 0$; $\frac{d\theta_e}{dt} = -2.645 \times 10^{-2} E$; and $\theta_e = \theta_{e_{(04)}}$:-

$$A_1 = -2.645 \times 10^{-2} E \quad (46)$$

$$A_2 = \theta_{e_{(04)}} - 1.96 \times 10^{-4} E \quad (47)$$

and equations (44) and (45) can be written

$$\frac{d\theta_e}{dt} = -2.645 \times 10^{-2} E\, e^{-135t} \quad (48)$$

$$\theta_e = \theta_{e_{(04)}} - 1.96 \times 10^{-4} E\,(1 - e^{-135t}) . \quad (49)$$

The current transient over this period, from equations (25), (41), (42) and (49) is:-

$$i = 0.001146\,\theta_e = 12.05 \times 10^{-4} - \left\{3.03t_{34} + 2.245\,(1 - e^{-135t})10^{-2}\right\} 10^{-5} E . \quad (50)$$

It will be noted from equations (49) and (50) that the final steady-state values of θ_e and i are given by:-

$$\theta_{e(s)} = \theta_{e_{(04)}} - 1.96 \times 10^{-4} E \quad (51)$$

$$i_{(s)} = 12.05 \times 10^{-4} - \left\{3.03t_{34} + 2.245 \times 10^{-2}\right\} 10^{-5} E . \quad (52)$$

The motion of the relay armature is given by equation (28), as the centralizing spring only is acting, and by inserting the current transient from (50):-

$$\frac{d^2\psi}{dt^2} + 2\sqrt{8}\,\frac{d\psi}{dt} + 8\psi = Z_1\, e^{-135t} + Z_2 \quad (53)$$

where $$Z_1 = 0.2875 \times 10^{-2} E \quad (54)$$

and $$Z_2 = 15.42 - (0.388t_{34} + 0.2875 \times 10^{-2}) E . \quad (55)$$

Solution of this equation gives:-

$$\psi = \left\{A_5 t + A_6\right\} e^{-\sqrt{8}t} + \frac{Z_1\, e^{-135t}}{17569} + \frac{Z_2}{8} \quad (56)$$

and:-

$$\frac{d\psi}{dt} = \left\{A_5 (1 - \sqrt{8}t) - \sqrt{8}\, A_6\right\} e^{-\sqrt{8}t} - \frac{135\, Z_1\, e^{-135t}}{17569} . \qquad (57)$$

Inserting conditions at t_{04} where $\psi = 0.008$; $t = 0$; and $\frac{d\psi}{dt} = \frac{d\psi}{dt}_{(t_{04})}$; then:-

$$A_6 = 0.008 - \frac{Z_1}{17569} - \frac{Z_2}{8} \qquad (58)$$

and

$$A_5 = \frac{d\psi}{dt}_{(t_{04})} + \sqrt{8}\, A_6 + \frac{135\, Z_1}{17569} . \qquad (59)$$

The final steady state value to which ψ tends, as $t \to \infty$, is obtained from equation (56):-

$$\psi_{(s)} = \frac{Z_2}{8} = 1.9275 - \{0.0485\, t_{34} + 0.359375 \times 10^{-3}\}\, E. \qquad (60)$$

Referring back to equation (52), it is evident that a necessary condition for the requirement of no overshoot is that $i_{(s)} > -i_o$, and the limit of this condition is $i_{(s)} = -i_o = -5 \times 10^{-6}$. Inserting this value into equation (52) gives the relationship:-

$$E = \frac{121}{3.03\, t_{34} + 2.245 \times 10^{-2}} . \qquad (61)$$

Equations (61) and (39) are both relationships between E and t_{34}, and by substitution the value of t_{34} is contained in the relationship:-

$$e^{-\sqrt{8}t_{34}} \sin (15.49 t_{34} - 0.361) - 0.1383 t_{34} + 0.466 = 0 . \qquad (62)$$

This gives

$$t_{34} = 3.369 \text{ seconds} \qquad (63)$$

and substitution into equation (61) gives:-

$$E = 11.825 \text{ volts} . \qquad (64)$$

Inserting these values of E and t into equations (40), (54), (55), (58) and (59) gives:-

$$\frac{d\psi}{dt}_{(t_{04})} = -0.0185 \text{ radians/sec} \qquad (65)$$

$$Z_1 = 0.034 \qquad (66)$$

$$Z_2 = -0.064 \qquad (67)$$

$$A_6 = 0.016 \qquad (68)$$

$$A_5 = 0.0271 . \qquad (69)$$

These numerical values inserted into equation (56) make:-

$$\psi = \{0.0271t + 0.016\}\, e^{-\sqrt{8}t} + \frac{0.034\, e^{-135t}}{17569} - 0.008 \qquad (70)$$

as the motion of the armature from instant t_{04} onwards. Also, equation (57) becomes:-

$$\frac{d\psi}{dt} = -\{0.0181 + 0.0765\}\, e^{-\sqrt{8}t} - 0.000261\, e^{-135t} . \qquad (71)$$

From inspection, $\frac{d\psi}{dt}$ is always negative, and tends to zero as $t \to \infty$. Therefore, there is no instant like t_{05} giving a $\psi_{(min)}$ value where $\frac{d\psi}{dt}$ is zero. Therefore in this case the characteristic of ψ follows the dotted line shown in Fig.9, and approaches the $-\psi_o$ line asymptotically from above.

Thus the value of $E = 11.825$ volts gives the optimum condition of operation without overshoot of indication, and from equation (22), the maximum error correction rate is

$$|\omega| = 0.314 \text{ radians/sec} . \qquad (72)$$

3 With Feedback

Fig.10 illustrates the transient behaviour of the system under the same conditions as Fig.9, except that feedback effects are now included, and prior to instant t_{06} it is assumed an error has been established large enough for the error correction rate to saturate to its maximum value. Fig.10a shows the sensing coil current, which, if regarded as near-balance, is also proportional to the error "θ_e" (see equation 25). The moving coil relay armature is now actuated by two current torques, one due to the current "i" in the sensing coil, and the other in opposition due to a current "i_f" in the feedback coil which is shown in Fig.10b. The effective current shown in Fig.10c can be taken as $(i - ni_f)$ where "n" is the ratio of turns of the feedback coil to the sensing coil.

At instant t_{06} the rate of error correction is given by equation (22), and from (25):-

$$\frac{di}{dt} = 0.001146 \frac{d\theta_e}{dt} \qquad (73)$$

giving

$$\frac{di}{dt}_{(max)} = -0.001146\, \omega = -3.03 \times 10^{-5} E_f \text{ amps/sec} . \qquad (74)$$

The effective current "$i - ni_f$" has just reached the value $+i_1 = 12.05 \times 10^{-4}$ amps, (see equation 31) and the moving coil relay armature starts to move from its "$+\psi_1$" position in accordance with equation (29), the effective current now being used. Thus:-

$$\frac{d^2\psi}{dt^2} + 2\sqrt{\frac{S_1}{J_r}}\frac{d\psi}{dt} + \frac{S_1 + S_2}{J_r}\psi = \frac{k_4}{J_r}(i - ni_f) + \frac{S_2\, \psi_o}{J_r} \qquad (75)$$

describes the motion over range $+\psi_1 > \psi > +\psi_o$. This becomes:-

$$\frac{d^2\psi}{dt^2} + 2\sqrt{8}\frac{d\psi}{dt} + 248\psi = 1.28 \times 10^4 (i - ni_f) + 1.32 . \qquad (76)$$

The effective current transient over the period t_{06} to t_{07} (called t_{67}) is:-

$$(i - ni_f) = i_1 - t\left|\frac{di}{dt}_{(max)}\right| ,$$

which from equation (32) becomes

$$(i - ni_f) = 12.05 \times 10^{-4} - 3.03 \times 10^{-5} E_f t . \qquad (77)$$

Substitution back into (76) gives:-

$$\frac{d^2\psi}{dt^2} + 2\sqrt{8}\frac{d\psi}{dt} + 248\psi = 17.34 - 0.388 E_f t$$

which is identical with equation (33). Following through the same steps as previously, equations (37) and (38) also describe the armature motion over interval t_{67}, and if $\frac{d\psi}{dt}$ at t_{07} is called $\frac{d\psi}{dt}_{(t_{07})}$, we have, from equations (39) and (40):-

$$E_f \left\{1.012 \times 10^{-4} e^{-\sqrt{8}t_{67}} \sin(15.49t_{67} - 0.361) - 1.565 \times 10^{-3} t_{67} + 3.57 \times 10^{-5}\right\} + 0.062 = 0 \qquad (78)$$

and:-

$$\frac{d\psi}{dt}_{(t_{07})} = -E_f \left\{1.012 \times 10^{-4} \times 15.75\, e^{-\sqrt{8}t_{67}} \sin(15.49t_{67} - 1.75) + 1.565 \times 10^{-3}\right\} . \qquad (79)$$

With feedback, the servomotor is required to operate at its maximum rating, and it is convenient here to insert the rated value of:-

$$E_f = 24 \text{ volts} . \qquad (80)$$

Inserting this value into equations (78) and (79) gives:-

$$t_{67} = 1.67 \text{ seconds} \qquad (81)$$

and

$$\frac{d\psi}{dt}_{(t_{07})} = -0.0375 \text{ rads/sec} . \qquad (82)$$

Instant $t_{(07)}$, when ψ reaches the value $+\psi_0 = 0.008$ rads, can be regarded as the beginning of a new transient period during which the motor commences to slow down, and during which the feedback current is zero. At t_{07} the effective current prior to the step change is given by equation (41):-

$$(i - ni_f)_{(07)} = 12.05 \times 10^{-4} - 3.03 \times 10^{-5} E_f t_{67} \quad (83)$$

and after the step change:-

$$i_{(07)} = 12.05 \times 10^{-4} - 3.03 \times 10^{-5} E_f t_{67} + ni_f . \quad (84)$$

This is clearly dependent on the value of ni_f, and for purposes of this argument is assumed to be adjusted to:-

$$ni_f = + i_o - \{12.05 \times 10^{-4} - 3.03 \times 10^{-5} E_f t_{67}\} \quad (85)$$

making $$i_{(07)} = + i_o = 5 \times 10^{-6} \text{ amps} \quad (86)$$

immediately after the step change.

From equation (25):-

$$\theta_{e(07)} = \frac{i_{(07)}}{0.001146} = 4.37 \times 10^{-3} \text{ radians} . \quad (87)$$

By similar steps to those used in deriving equations (43) to (49), the error transient is given by:-

$$\theta_e = \theta_{e(07)} - 1.96 \times 10^{-4} E_f (1 - e^{-135t}) \quad (88)$$

and the current transient by:-

$$i = 0.001146 \theta_e = 5 \times 10^{-6} - 2.245 \times 10^{-7} E_f (1 - e^{-135t}) \quad (89)$$

following the dotted curve of Fig.10c from instant t_{07} onwards. The steady state of "i" as $t \to \infty$ is:-

$$i_{(s)} = 5 \times 10^{-6} - 2.245 \times 10^{-7} E_f = - 0.335 \times 10^{-6} \text{ amps} . \quad (90)$$

The movement of the relay armature from instant t_{07} onwards is given by equation (28), using the current relationship given by equation (89); thus:-

$$\frac{d^2\psi}{dt^2} + 2\sqrt{8}\frac{d\psi}{dt} + 8\psi = 1.28 \times 10^{-4} \left\{5 \times 10^{-6} - 2.245 \times 10^{-7} E_f (1 - e^{-135t})\right\}$$

or

$$\frac{d^2\psi}{dt^2} + 2\sqrt{8}\frac{d\psi}{dt} + 8\psi = 0.069 e^{-135t} - 0.005 . \quad (91)$$

Solution of this equation gives:-

$$\psi = \left\{A_7 t + A_8\right\} e^{-\sqrt{8}t} + \frac{0.069 e^{-135t}}{17569} - \frac{0.005}{8} \quad (92)$$

and:-

$$\frac{d\psi}{dt} = \{A_7 (1 - \sqrt{8}t) - \sqrt{8}\, A_8\}\, e^{-\sqrt{8}t} - \frac{135 \times 0.069\, e^{-135t}}{17569} \qquad (93)$$

where $A_8 = 0.0086$

and $A_7 = -0.0127$ (94)

from initial conditions at t_{07} where $\psi = \psi_0 = 0.008$, $t = 0$, and $\frac{d\psi}{dt} = \frac{d\psi}{dt}_{(t_{07})} = -0.0375$ (see equation 82).

Inserted into equation (93) gives:-

$$\frac{d\psi}{dt} = \{0.0359t - 0.037\}\, e^{-\sqrt{8}t} - 0.0005\, e^{-135t} . \qquad (95)$$

The second term is negligibly small and from inspection, the 'ψ' curve starts at t_{07} (where $t = 0$) with a negative slope, the numerical value of which progressively decreases, until at the value:-

$$t = \frac{0.037}{0.0359} = 1.03 \text{ seconds} \qquad (96)$$

the slope is zero. After this instant, the slope becomes positive and as $t \to \infty$, $\frac{d\psi}{dt} \to 0$. The "ψ" curve thus follows the dotted line shown on Fig.10d, and has a $\psi_{(min)}$ value at $t = 1.03$ seconds. Inserting this value into equation (92) gives the numerical result:-

$$\psi_{(min)} = -0.000846 \text{ radians} . \qquad (97)$$

This value does not reach the $-\psi_0$ limit of -0.008 radians, therefore there is no re-corrective action from the relay and thus no overshoot of indication. Referring to equation (74) the saturated error correction rate is now given by:-

$$\omega = \frac{3.03 \times 10^{-5} \times 24}{0.001146} = 0.634 \text{ rads/sec} \qquad (98)$$

and it is evident that, in this particular case, the saturated error correction rate could be still further increased (by increase of E_f) until $\psi_{(min)} = -0.008$.

Thus the comparative results of this servo system, for a requirement of no overshoot of indication are:-

Without feedback, maximum error correction rate = 0.314 rads/sec.

With feedback, " " " " > 0.634 rads/sec.

It will be noted that, in the actual instrument the maximum error correction rate has been adjusted to a slightly lower figure of 33.3°/sec or 0.581 rads/sec by lowering the motor voltage E_f to 22 volts. This rate has been found adequate in practice, and saves some of the wear and tear of the servo system and relay contacts. It is pointed out that this feedback adjustment (giving the above analysed conditions) is suited for

the position of maximum bridge sensitivity, and at other balanced positions, $\frac{di}{dt}$ being less, there may be several steps of feedback operation before final balance and these (occurring very rapidly) involve several quick change-over sequences from the relays, as shown in the recording in Fig.12b.

Wt.2078.CP.230.K3 - Printed in Great Britain.

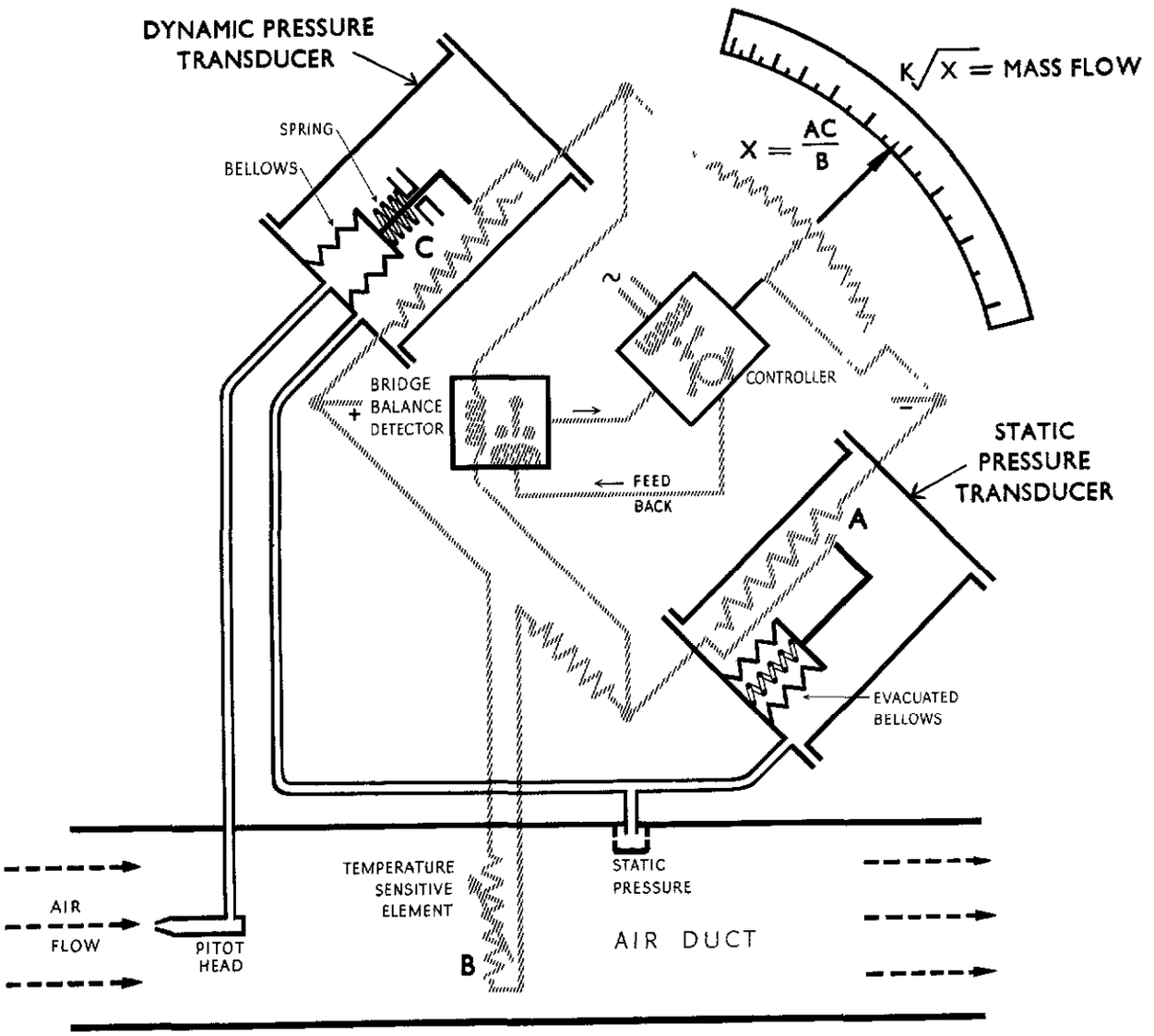

FIG.1. DIAGRAM OF METER

FIG.2 & 3

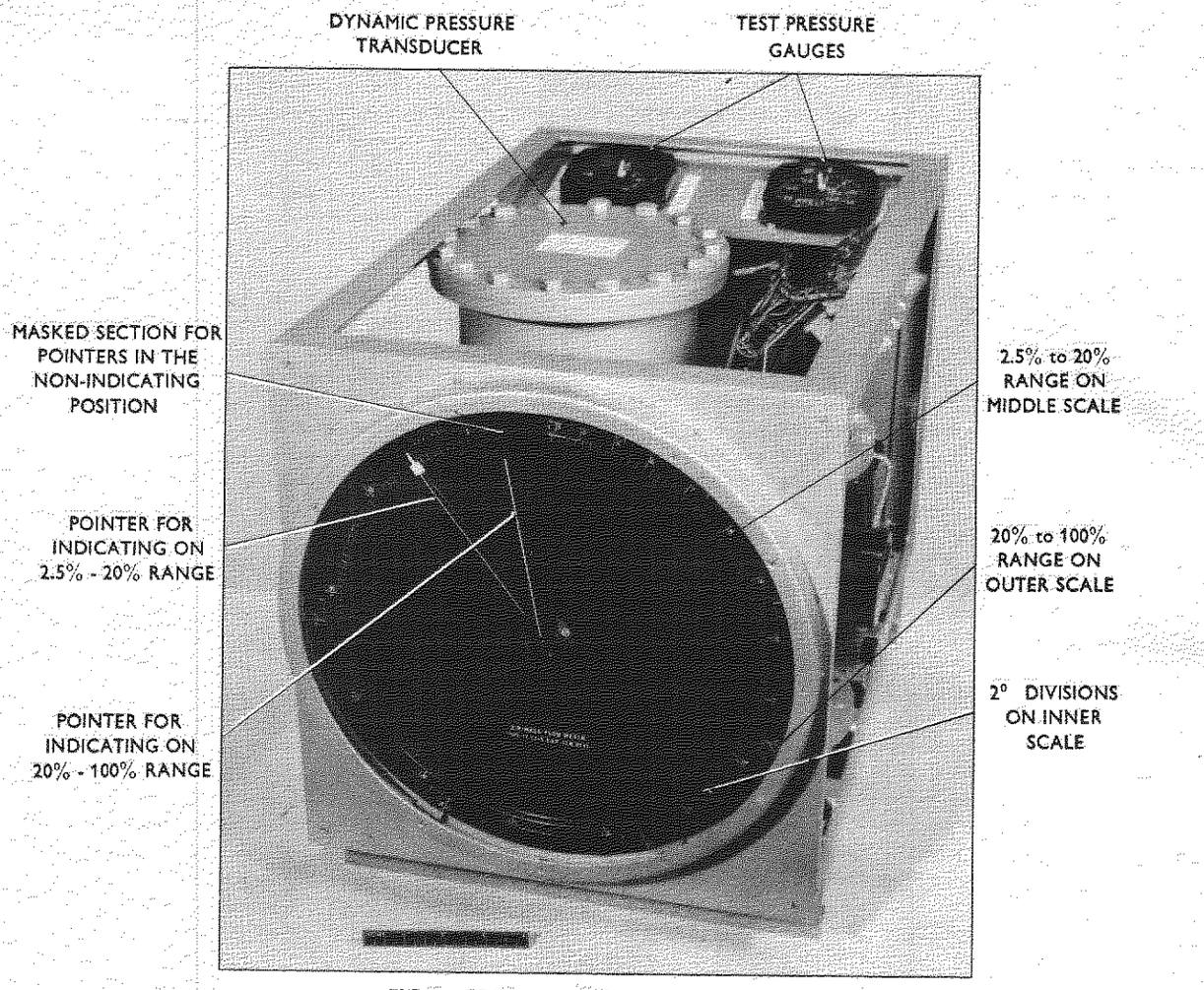

FIG.2. FRONT VIEW OF INSTRUMENT

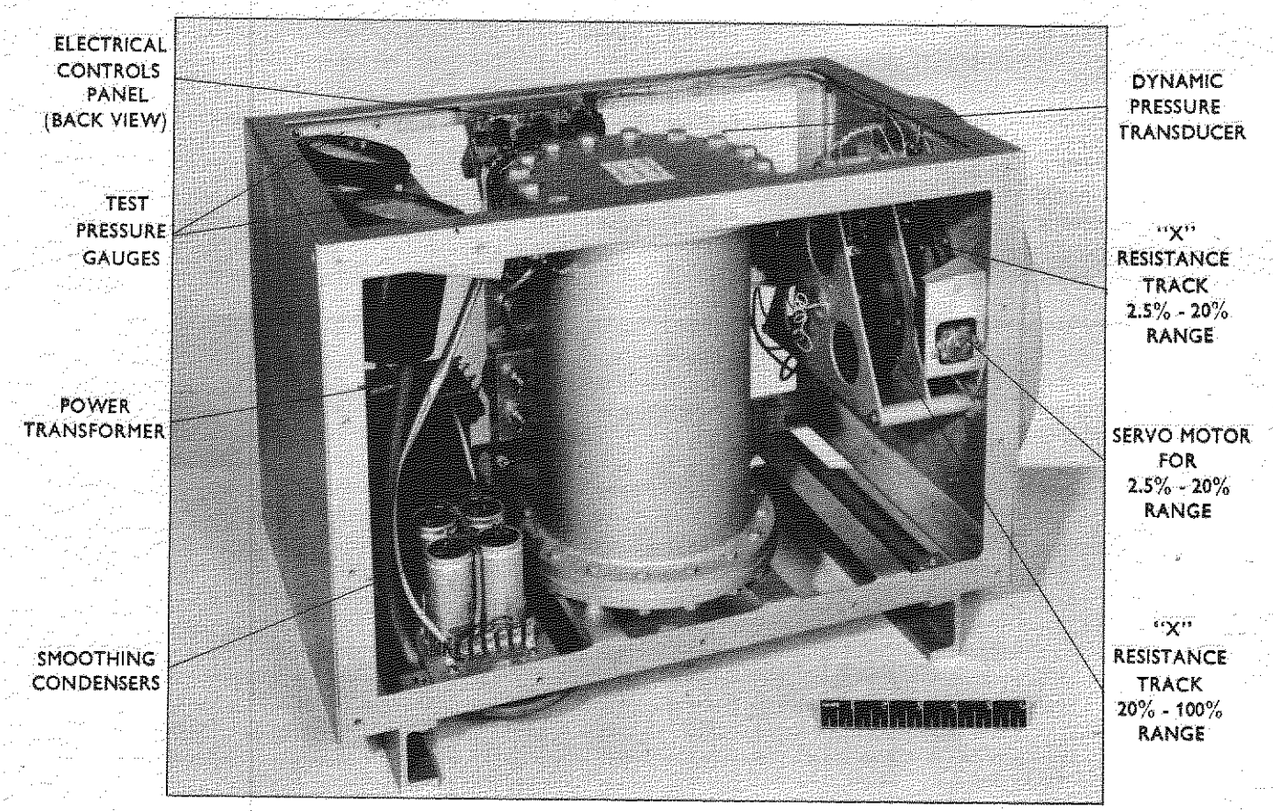

FIG.3. SIDE VIEW (LEFT HAND) OF INSTRUMENT

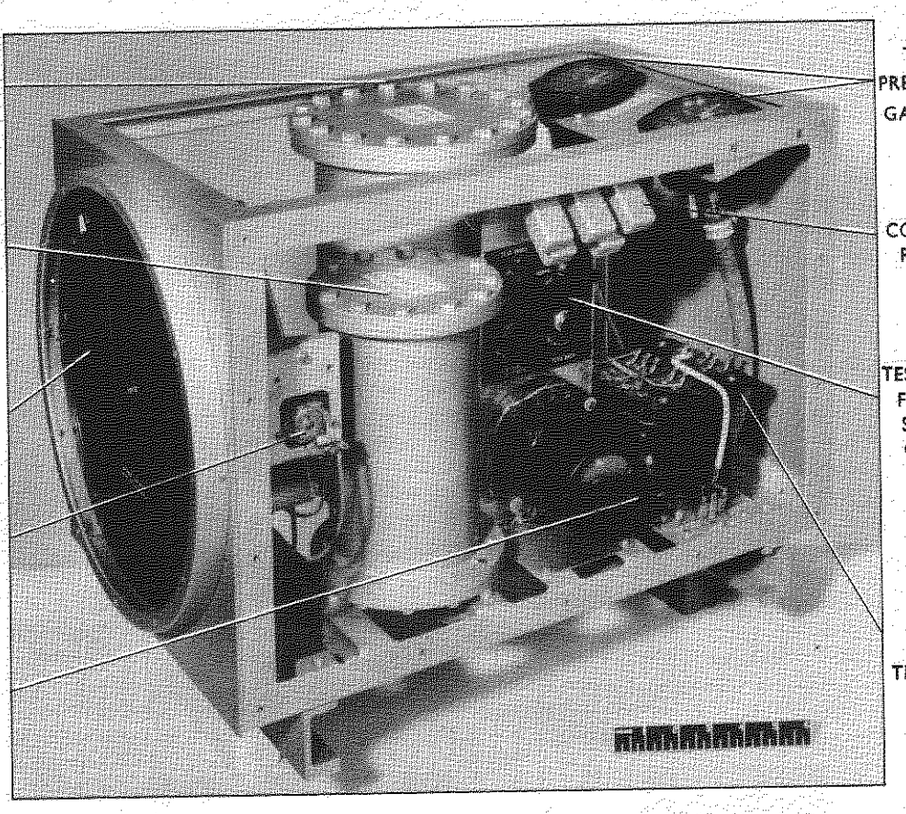

FIG.4. SIDE VIEW (RIGHT HAND) OF INSTRUMENT

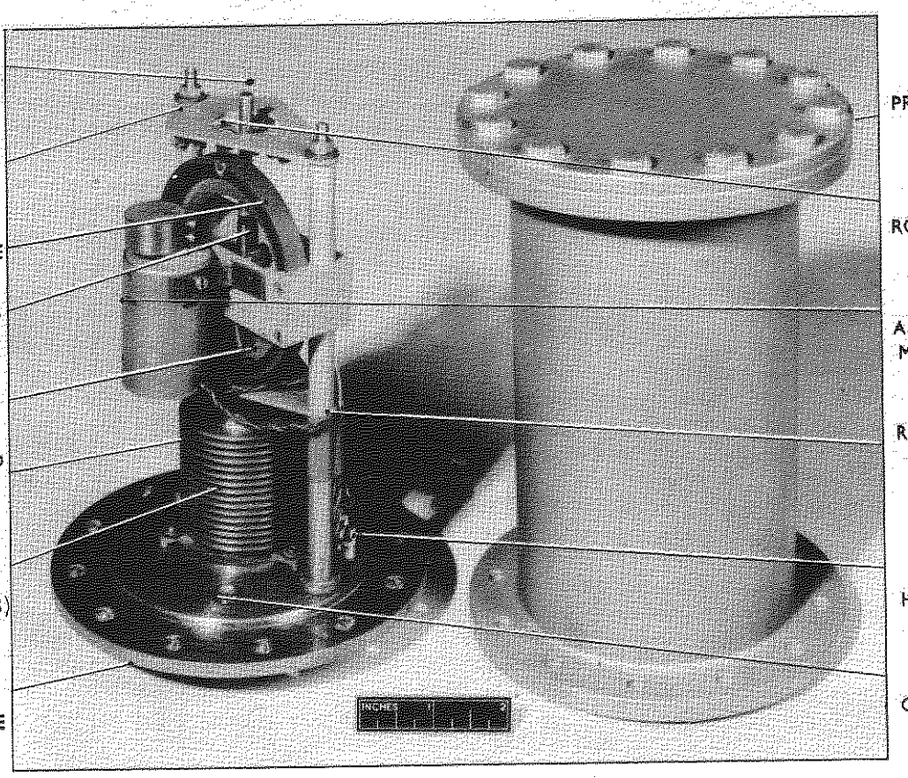

FIG.5. STATIC PRESSURE TRANSDUCER

FIG.6 & 7

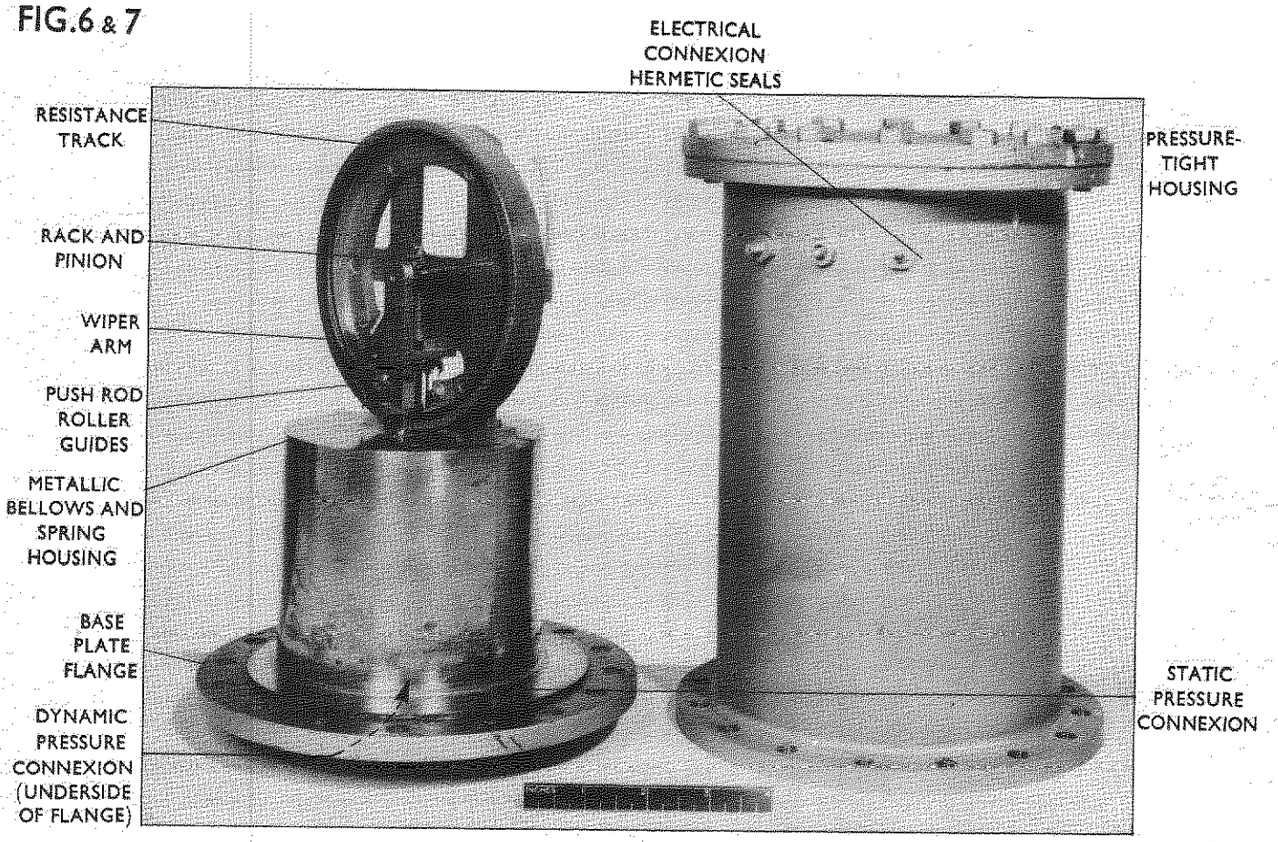

FIG.6. DYNAMIC PRESSURE TRANSDUCER

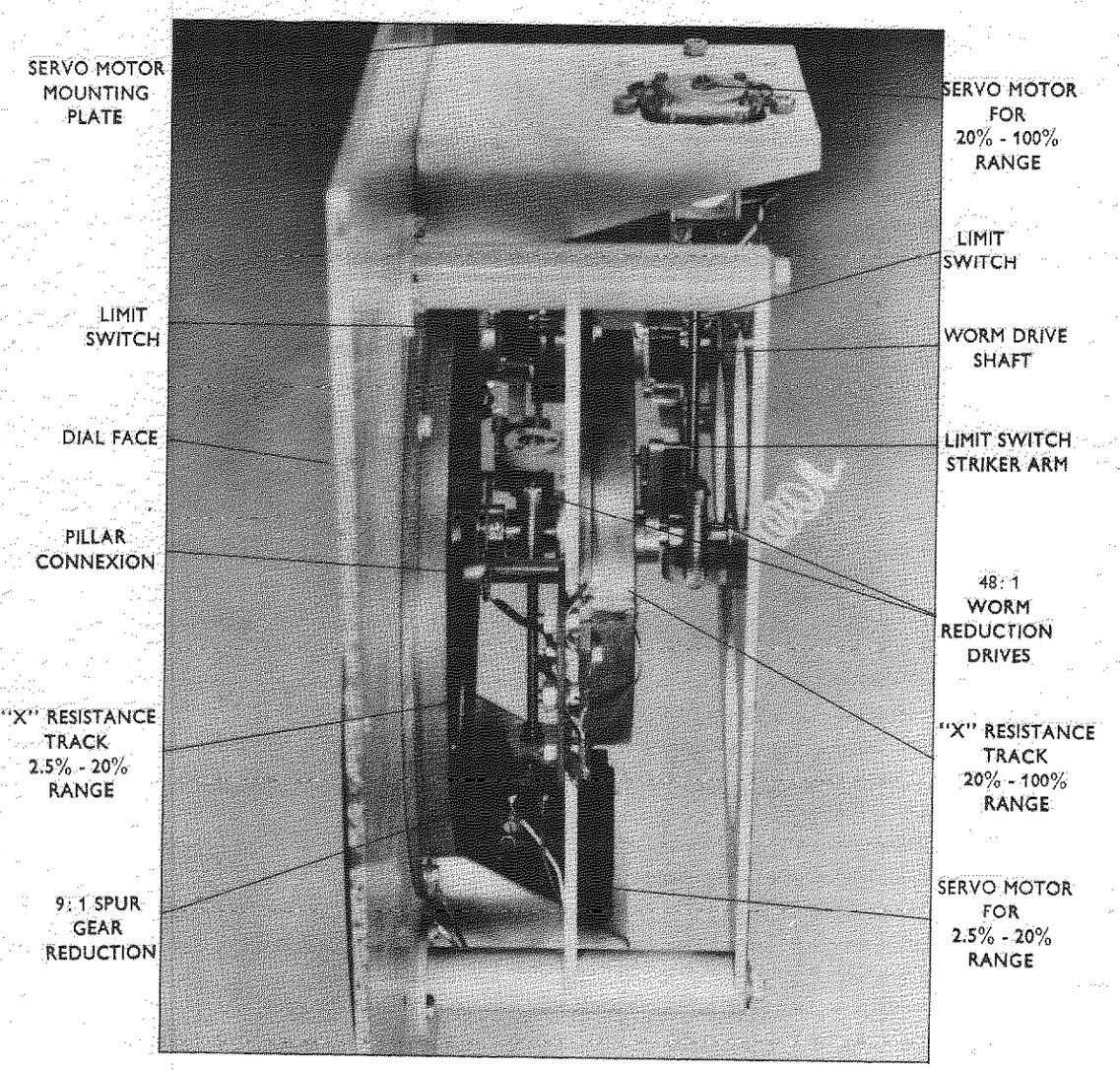

FIG.7. DIAL PLATE, SERVO MOTORS AND DRIVES ASSEMBLY

FIG.8.

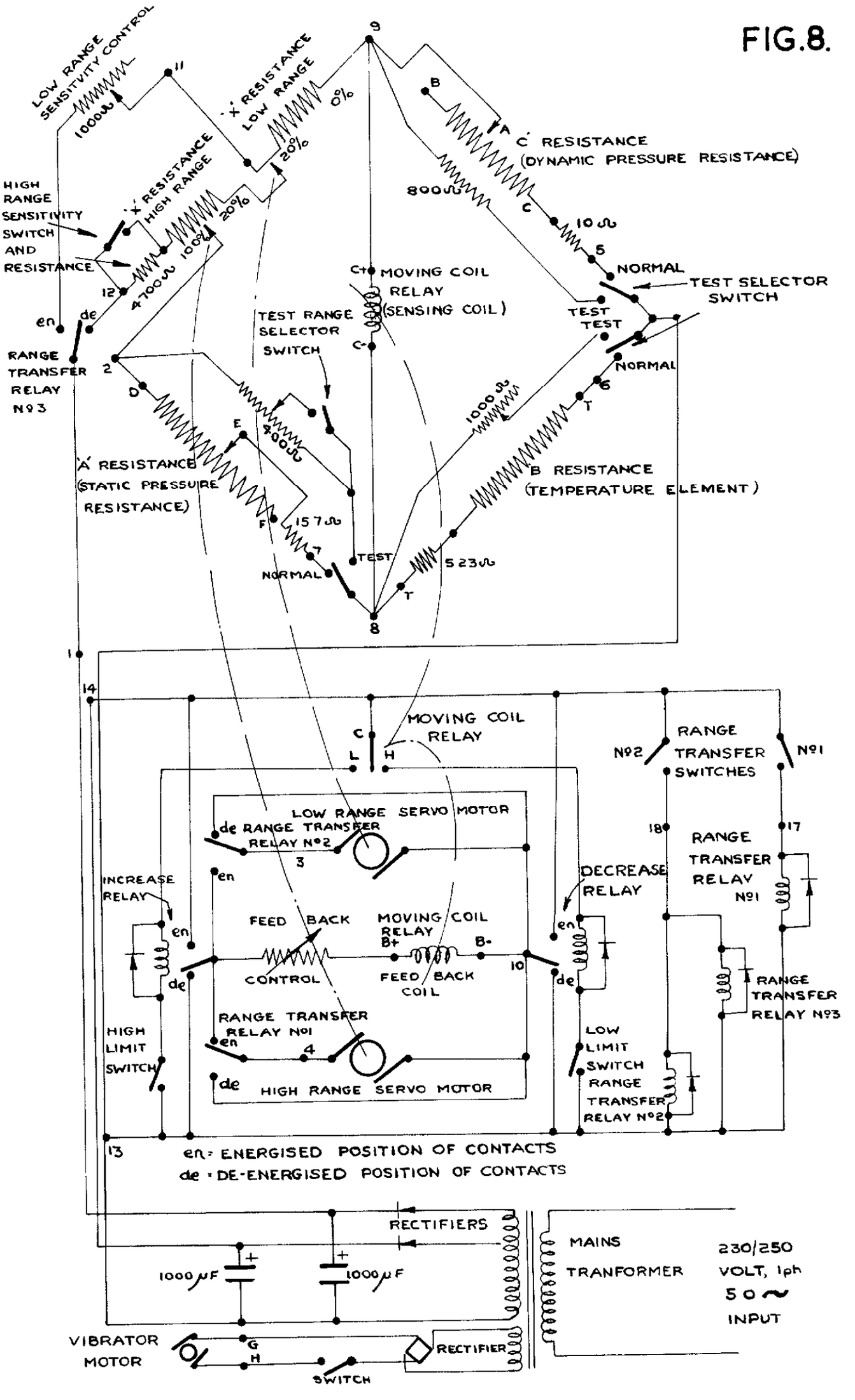

FIG.8. WIRING DIAGRAM

FIG.9.

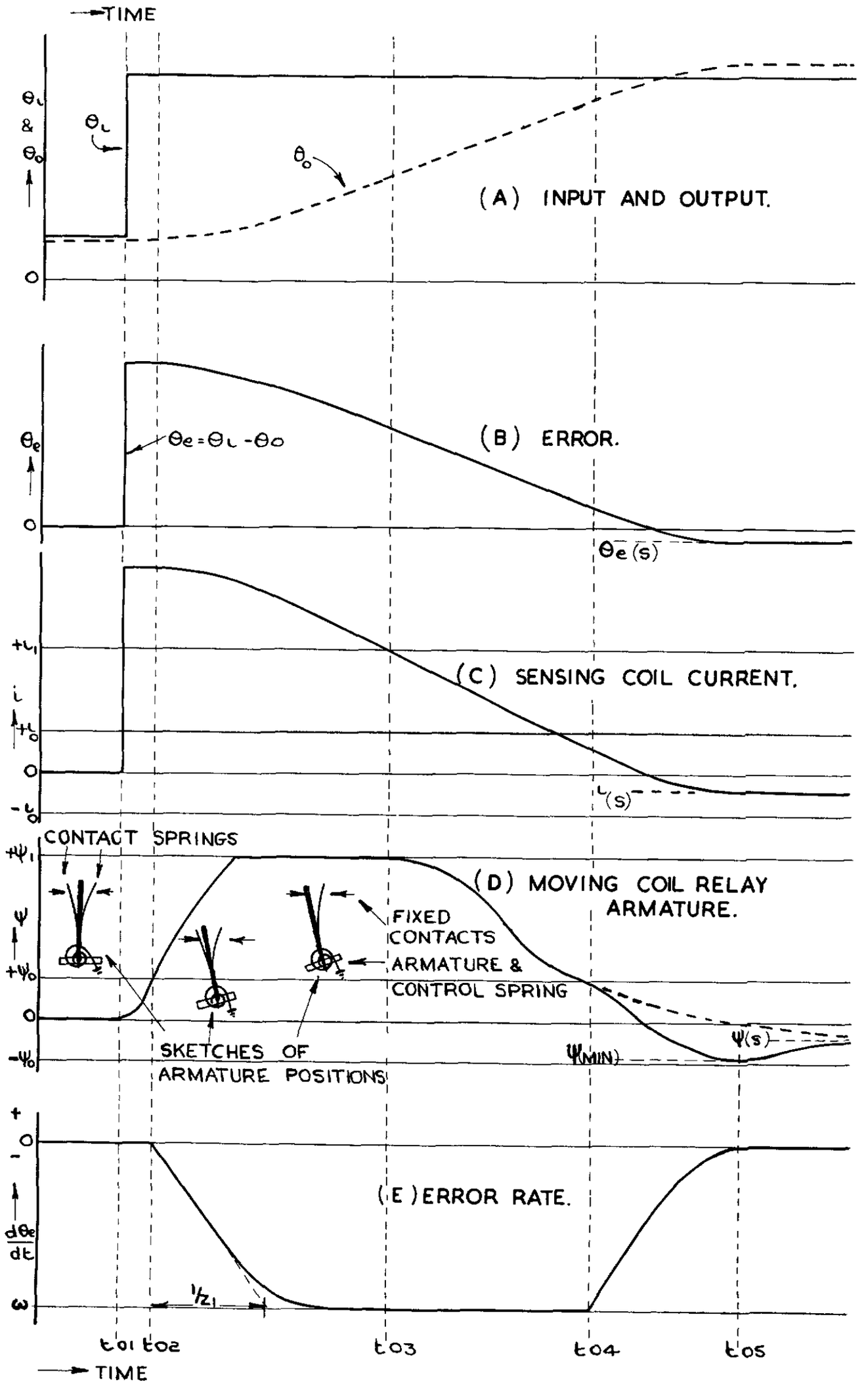

FIG.9. TRANSIENT BEHAVIOUR OF SERVO SYSTEM (WITHOUT SECONDARY FEEDBACK.)

FIG.10.

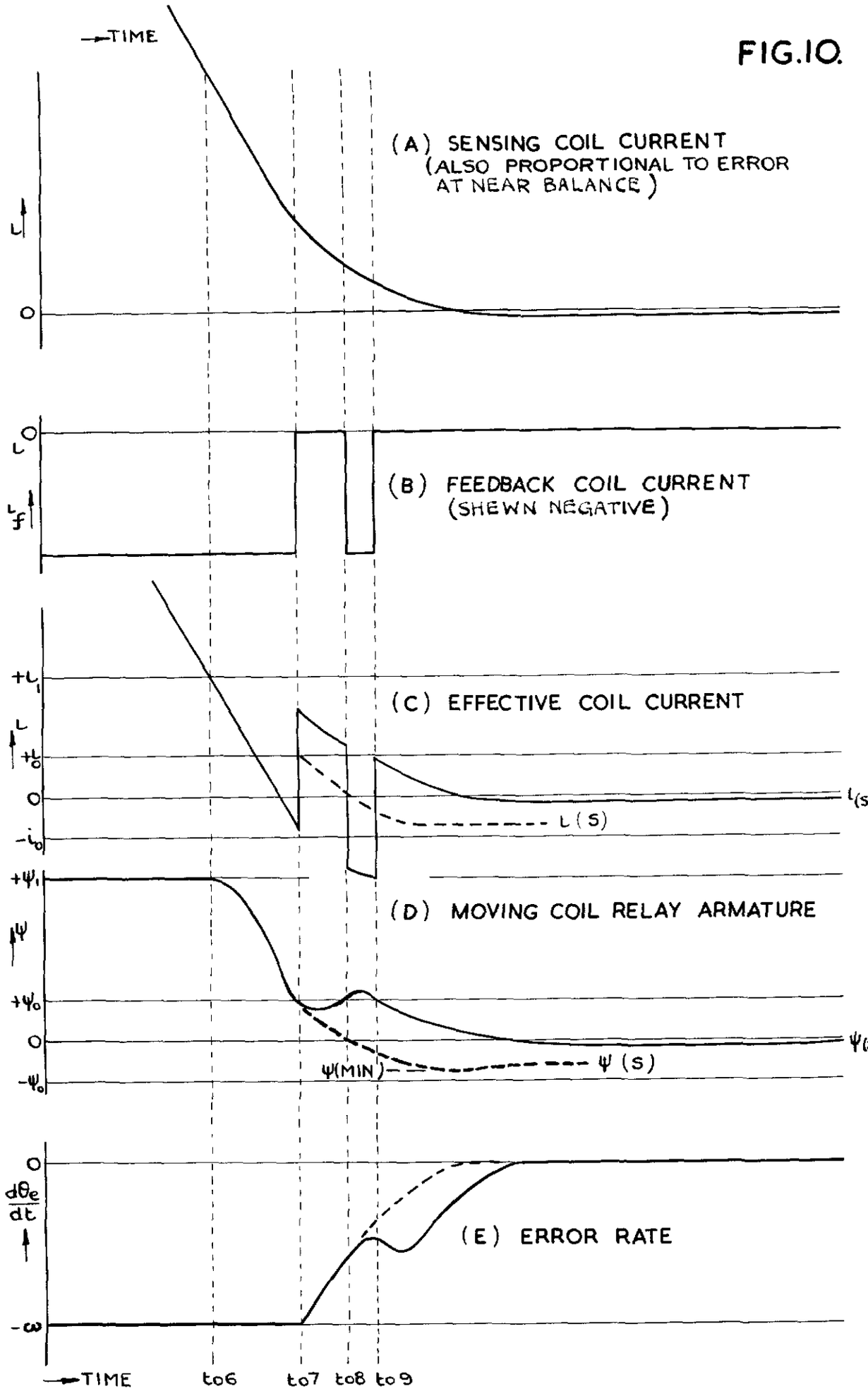

FIG. 10. TRANSIENT BEHAVIOUR OF SERVO SYSTEM (WITH SECONDARY FEEDBACK.)

FIG.11.

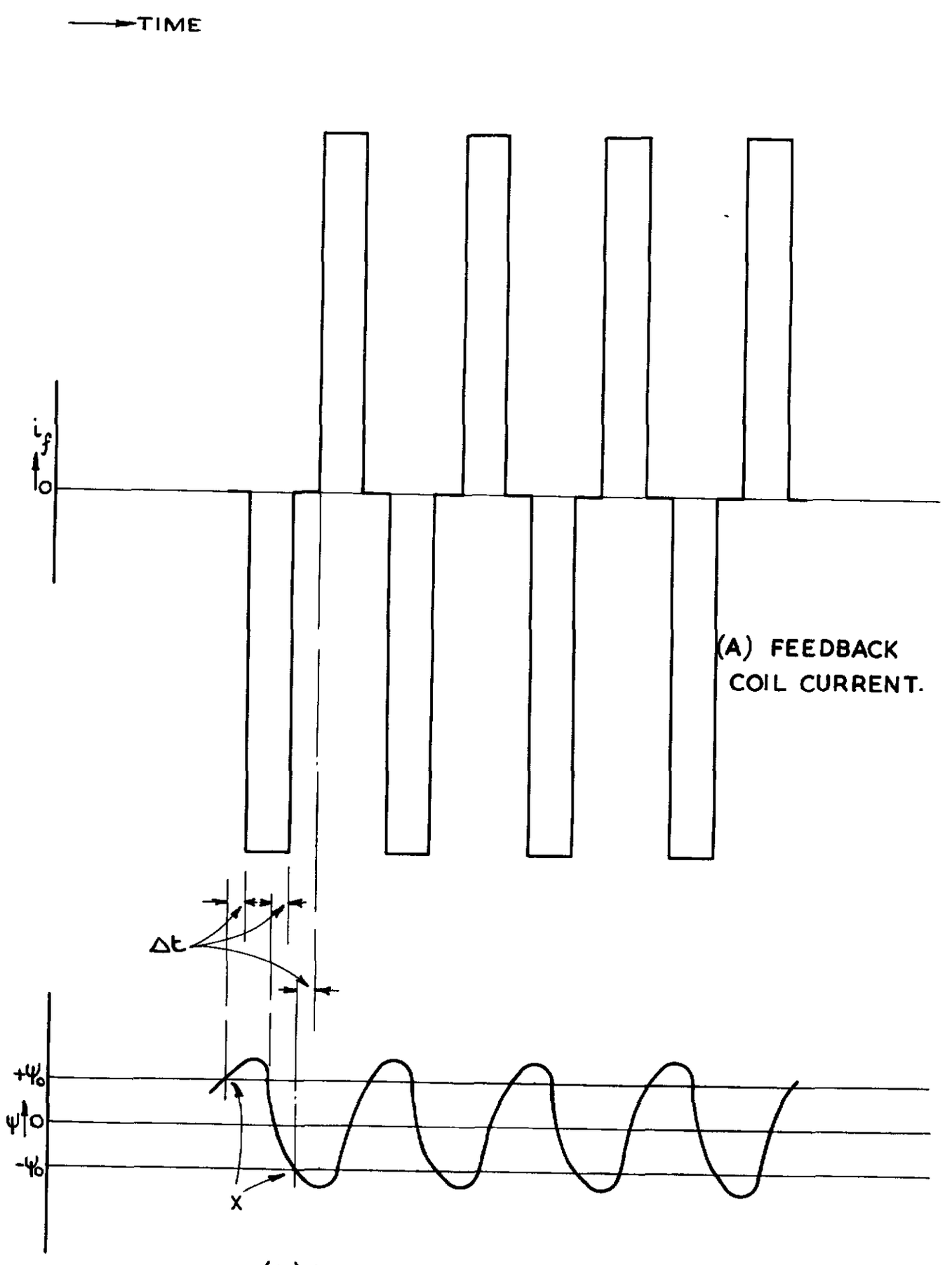

FIG.11. OSCILLATORY BEHAVIOUR OF RELAY DUE TO EXCESSIVE SECONDARY FEEDBACK.

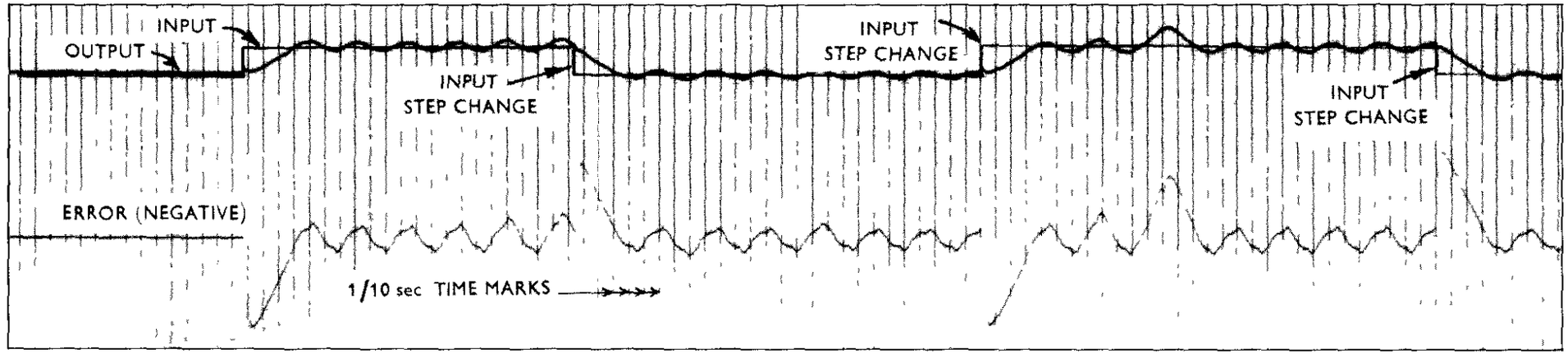

A. WITHOUT SECONDARY FEEDBACK

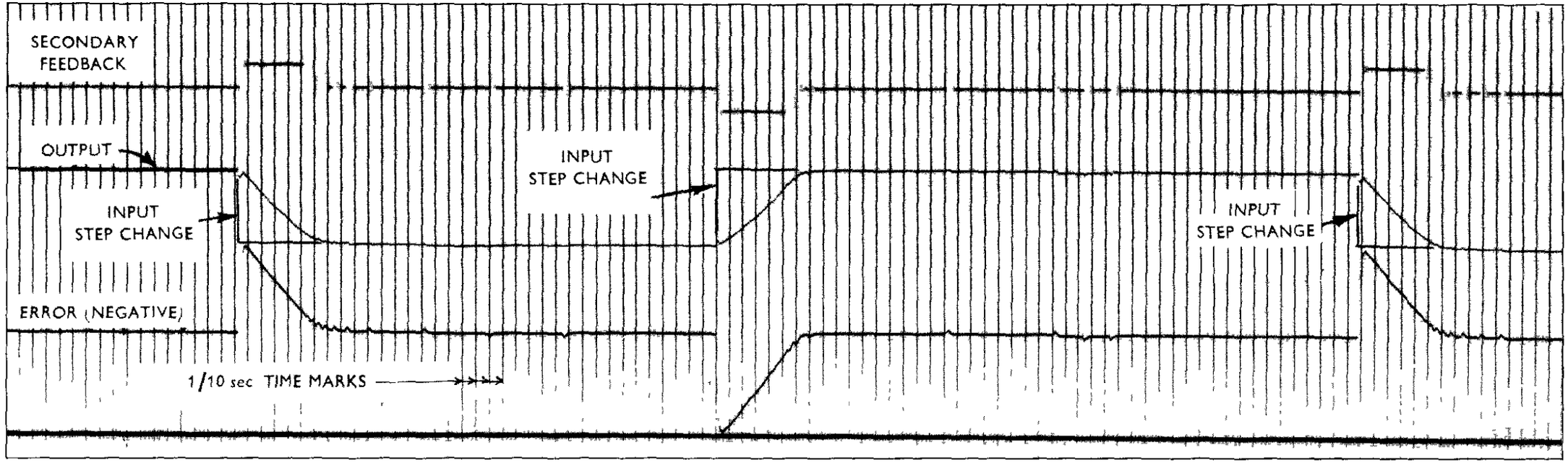

B. WITH SECONDARY FEEDBACK

FIG 12. RECORDING OF SERVO SYSTEM BEHAVIOUR

FIG. 12

FIG. 13

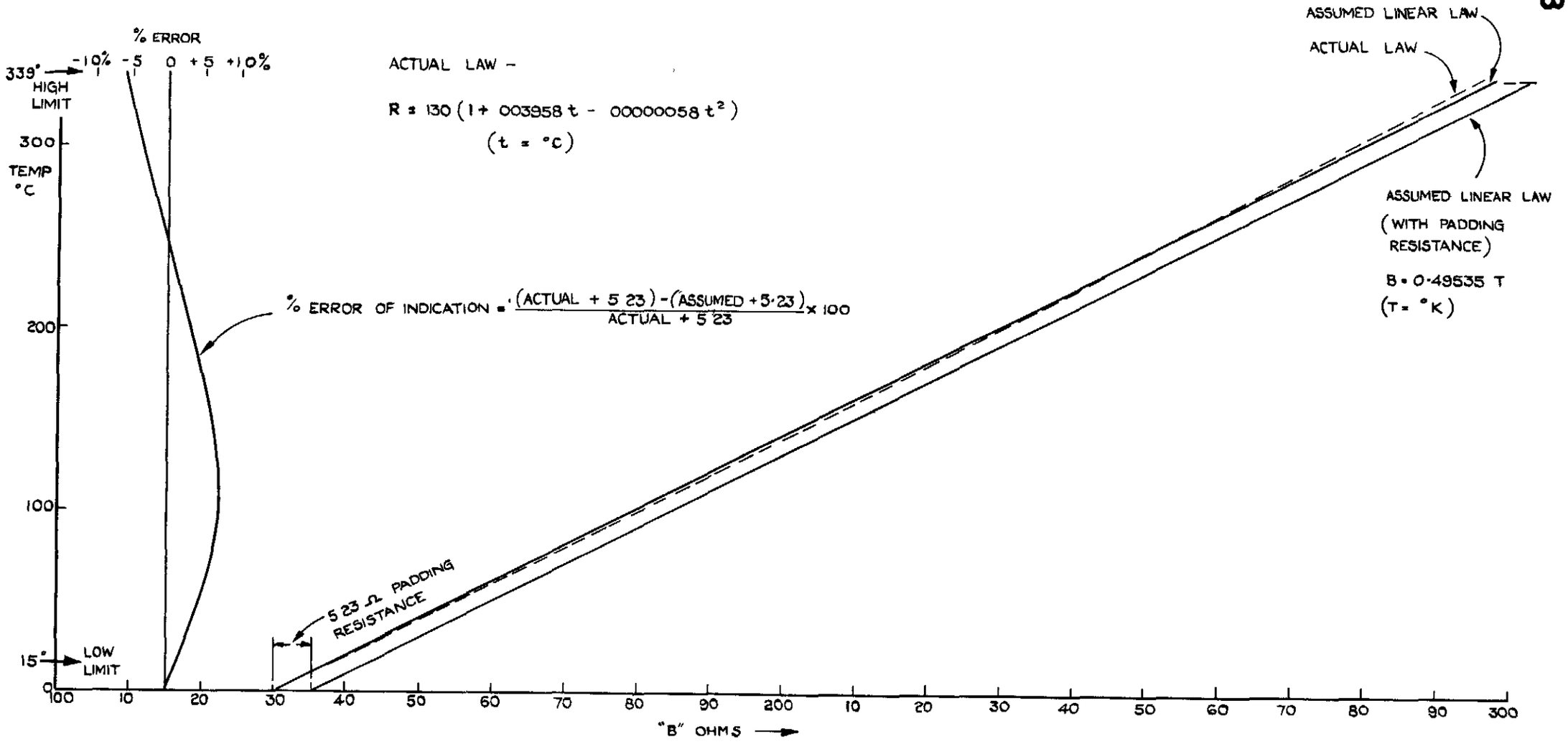

FIG. 13 PLATINUM IMPACT TYPE TEMPERATURE BULB. VARIATION OF RESISTANCE WITH TEMPERATURE.

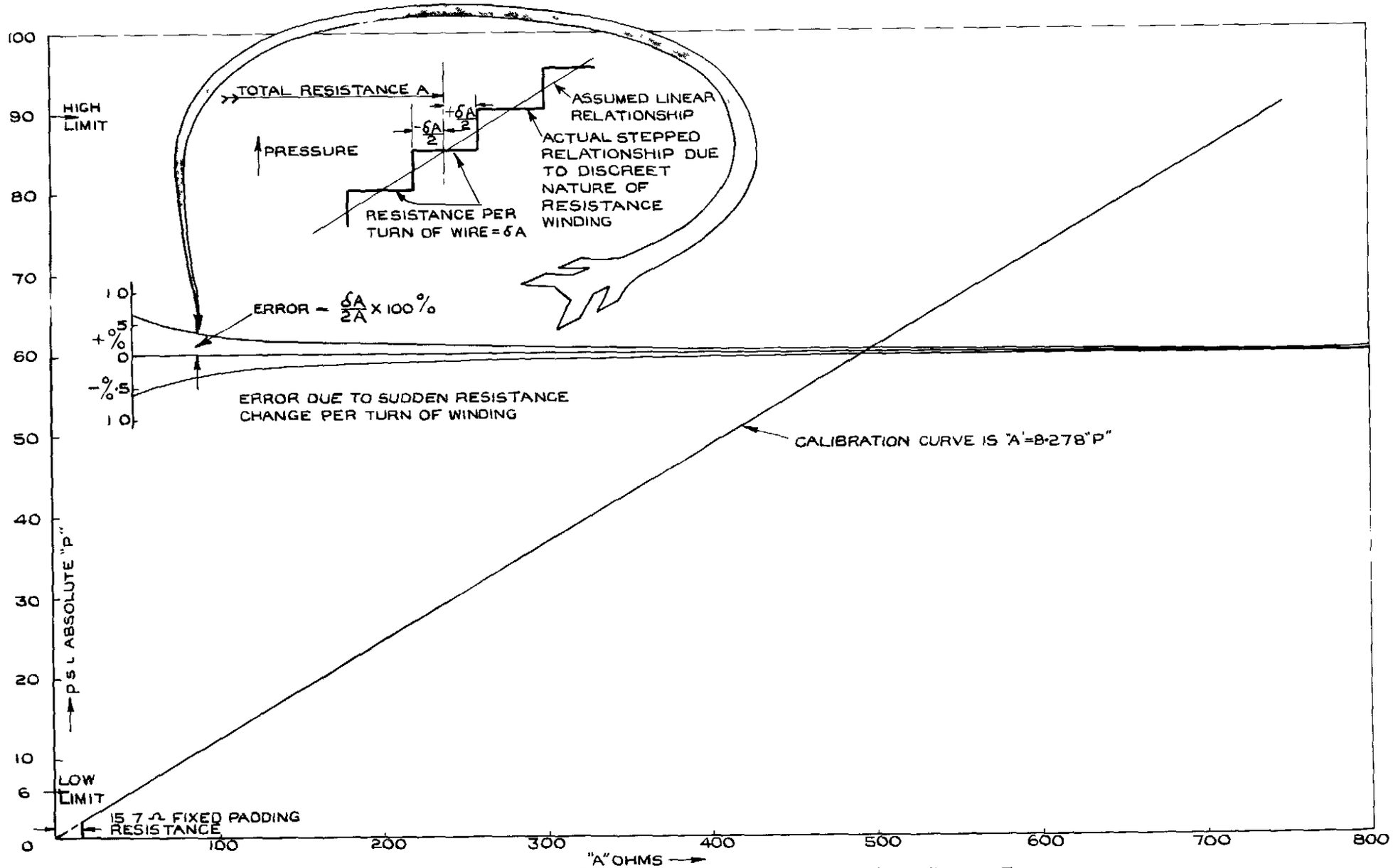

FIG 14 STATIC PRESSURE TRANSDUCER—VARIATION OF RESISTANCE WITH PRESSURE

FIG 14

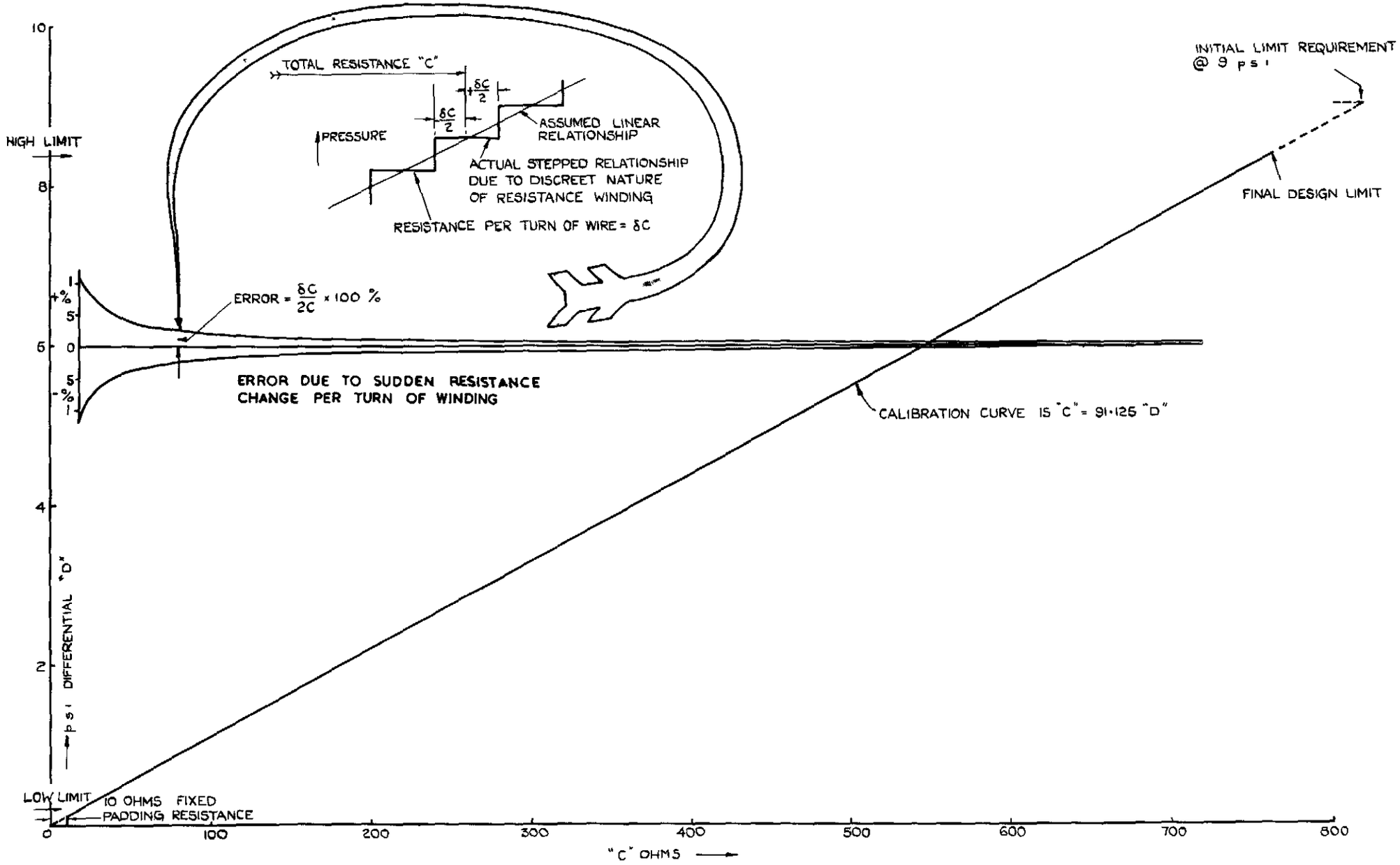

FIG. 15 DYNAMIC PRESSURE TRANSDUCER – VARIATION OF RESISTANCE WITH PRESSURE

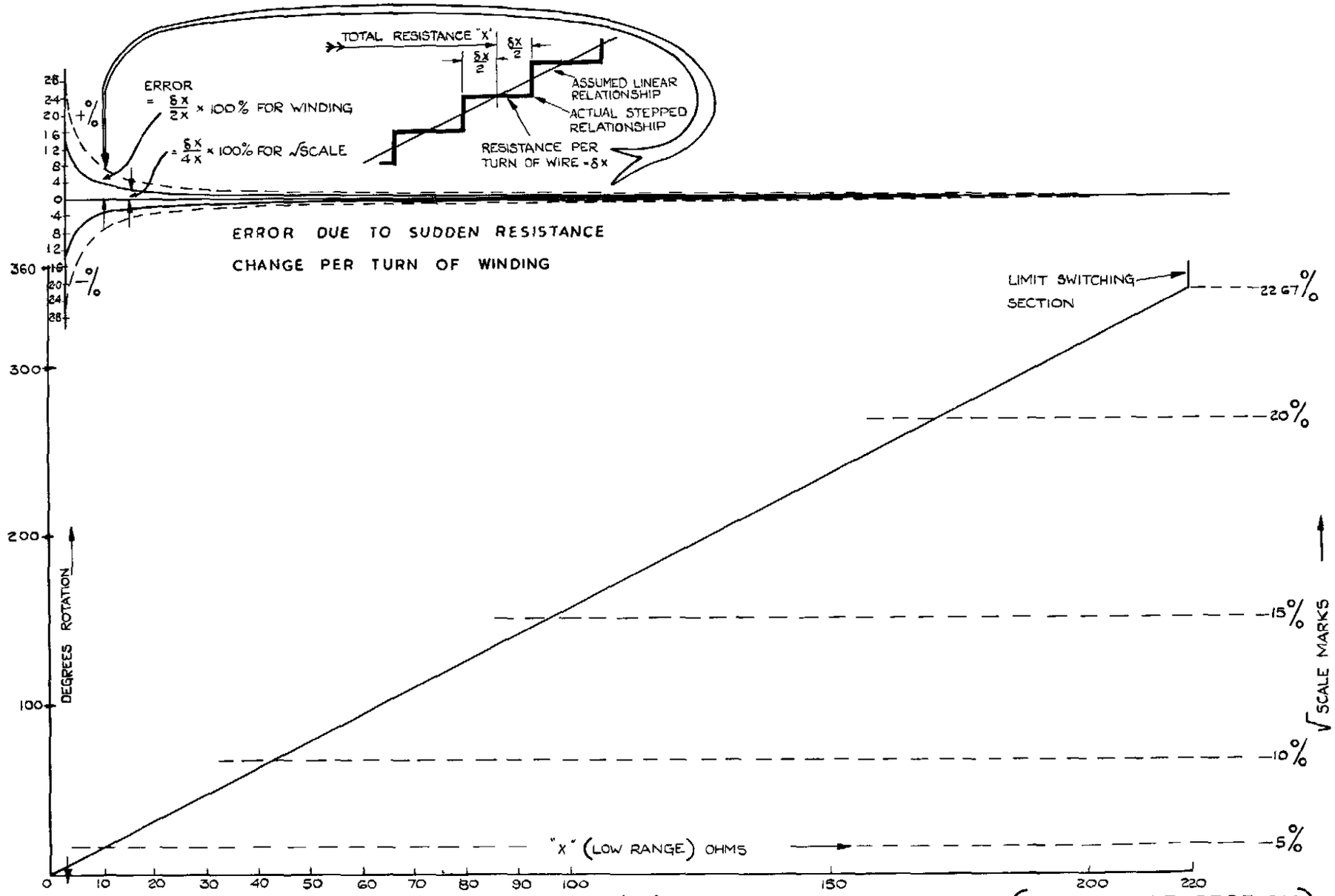

FIG 16 CALCULATED CHARACTERISTIC OF THE 'X' INDICATING RESISTANCE (LOW RANGE SECTION)

FIG 16

FIG. 17

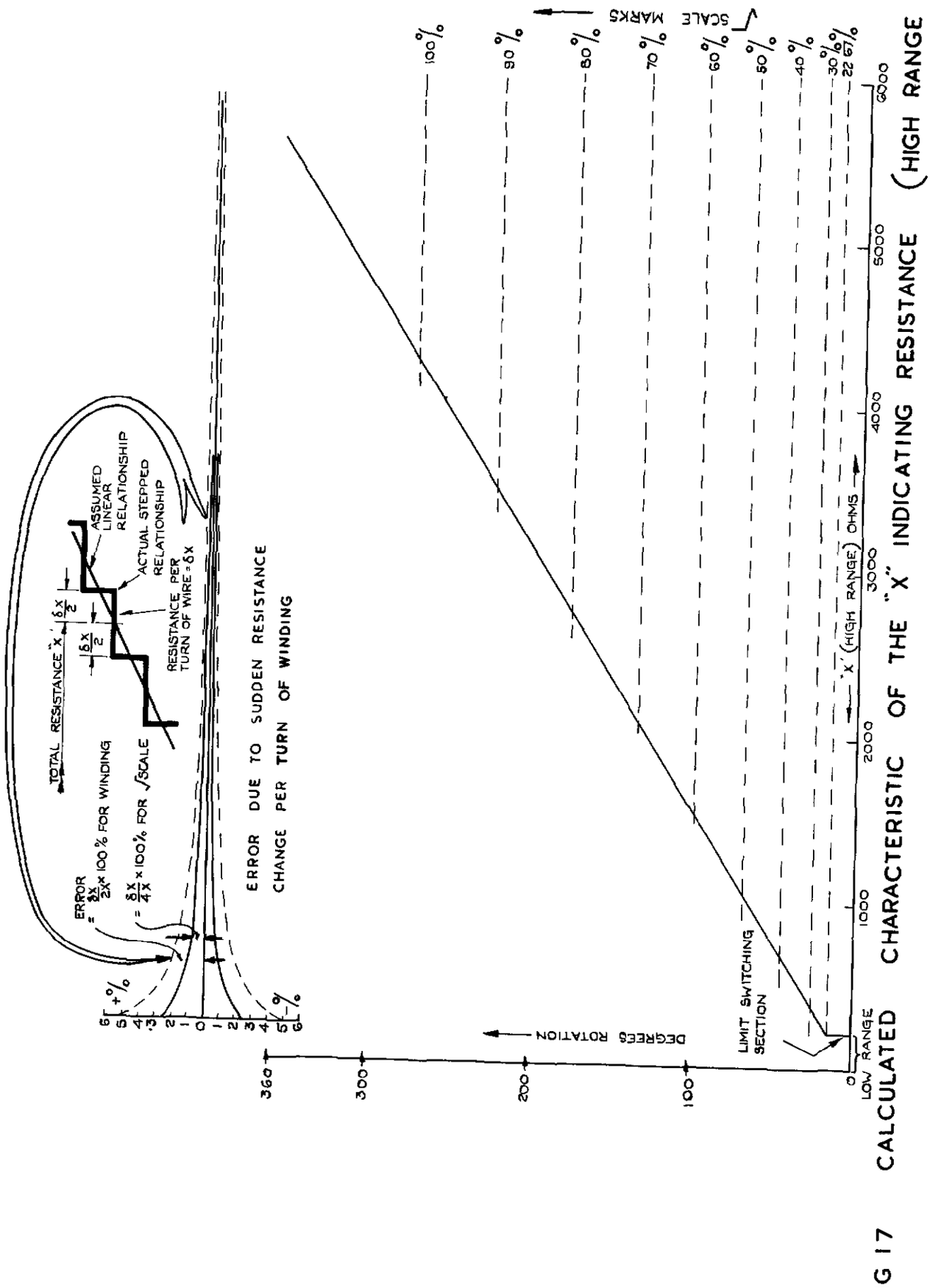
CALCULATED CHARACTERISTIC OF THE "X" INDICATING RESISTANCE (HIGH RANGE SECTION)
DEGREES ROTATION
360
300
200
100
0
LOW RANGE
LIMIT SWITCHING SECTION
1000
2000
3000
4000
5000
6000
"X" (HIGH RANGE) OHMS
SCALE MARKS
100%
90%
80%
70%
60%
50%
40%
30%
22 67%
ERROR DUE TO SUDDEN RESISTANCE CHANGE PER TURN OF WINDING
TOTAL RESISTANCE "X"
ASSUMED LINEAR RELATIONSHIP
ACTUAL STEPPED RELATIONSHIP
RESISTANCE PER TURN OF WIRE = δX
ERROR = δX/2X × 100% FOR WINDING
= δX/4X × 100% FOR √SCALE

FIG 17

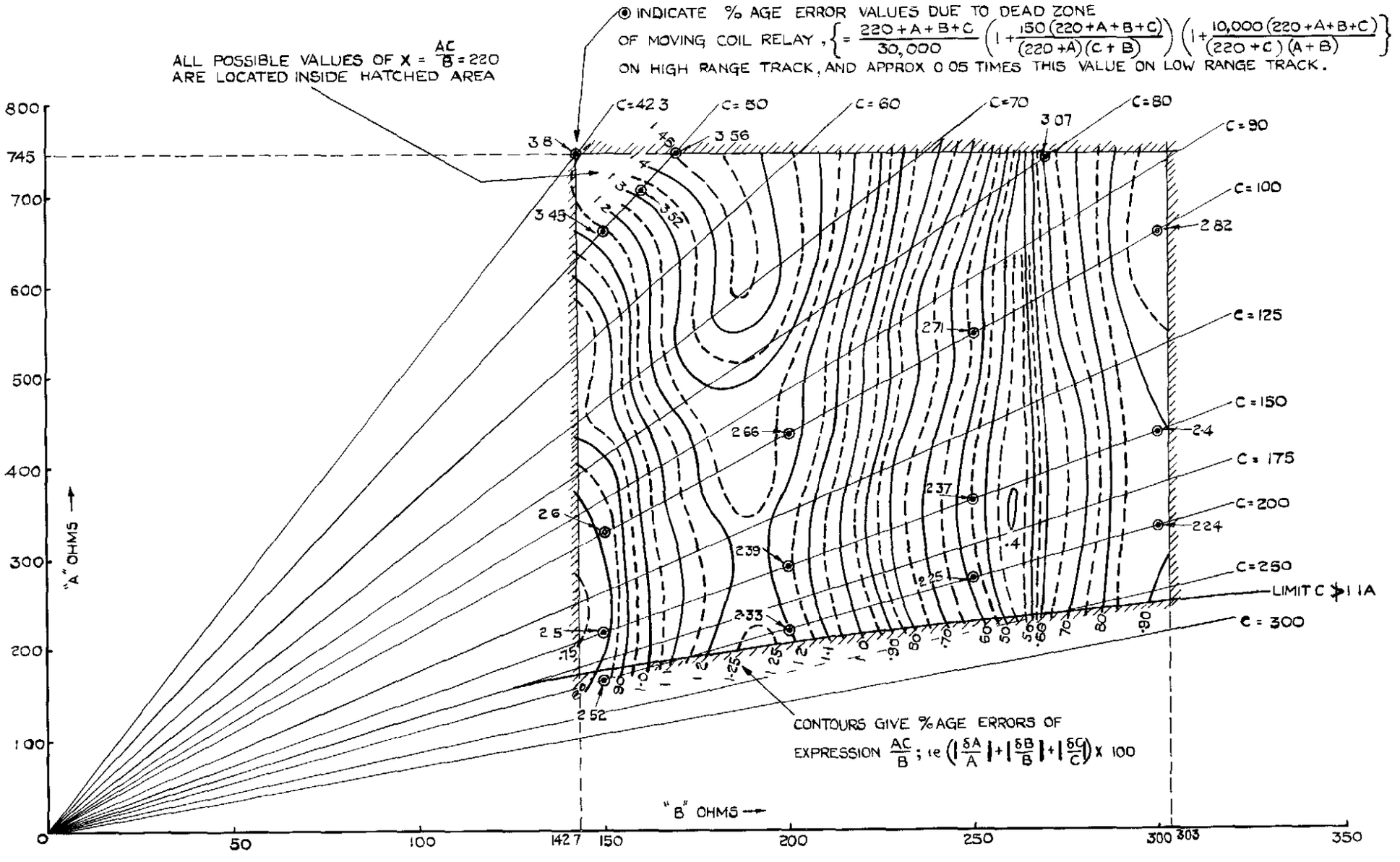

FIG. 18. DIAGRAM SHEWING ERROR DISTRIBUTION AT CHANGE-OVER POSITION OF TRACKS. (i.e. AT X = 220 OHMS.)

FIG. 18.

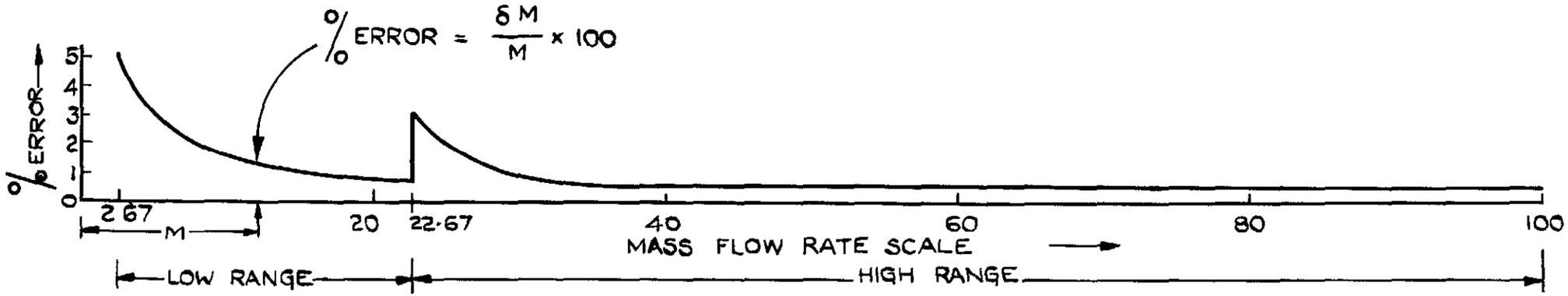

(a) EXPRESSED AS A %AGE OF THE ACTUAL MASS FLOW RATE.

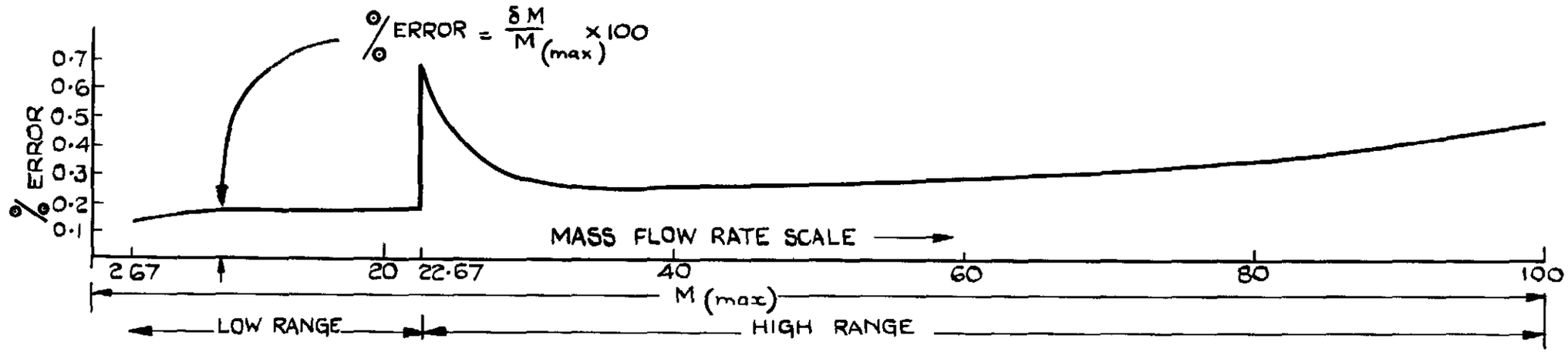

(b) EXPRESSED AS A % AGE OF THE MAXIMUM FLOW RATE.

FIG.19(a & b) ESTIMATED TOTAL MAXIMUM ERROR OF MASS FLOW RATE INDICATION.

C.P. No. 230
(17,696)
A.R.C. Technical Report

Published by
HER MAJESTY'S STATIONERY OFFICE
To be purchased from
York House, Kingsway, London W.C.2
423 Oxford Street, London W 1
P O Box 569, London S E 1
13A Castle Street, Edinburgh 2
109 St. Mary Street, Cardiff
39 King Street, Manchester 2
Tower Lane, Bristol 1
2 Edmund Street, Birmingham 3
80 Chichester Street, Belfast
or through any bookseller

PRINTED IN GREAT BRITAIN

S.O. Code No. 23-9009-30

Wt 2078.K3

C.P. No. 230